Matrix-Isolation FTIR Studies and Theoretical Calculations of Hydrogen-Bonded Complexes of Imidazole. A Comparison between Experimental Results and Different Calculation Methods

Marlies K. Van Bael,[†] Johan Smets,[†,‡] Kristien Schoone,[†] Linda Houben,[†] William McCarthy,[‡] Ludwik Adamowicz,[‡] Maciej J. Nowak,[§] and Guido Maes*[,†,||]

Department of Chemistry, University of Leuven, Celestijnenlaan 200F, B-3001, Heverlee, Belgium, Department of Chemistry, University of Arizona, Tucson, Arizona 85721, and Institute of Physics, Polish Academy of Sciences, Al. Lotnikow 32/46, 02-668 Warsaw, Poland

Received: November 6, 1996[⊗]

The hydrogen bond interaction between water and imidazole was investigated with the matrix-isolation FTIR spectroscopy coupled to *ab initio* calculations performed with the RHF and MP2 methods and the parametrized DFT method with the B3LYP hybrid functional. The 6-31G** and 6-31++G** basis sets were used in the calculations. Evaluation of the accuracy of the three methods and the two basis sets was made for noncomplexed imidazole. All three of the methods gave geometries for imidazole in good agreement with the experimental structure. Also, all three levels of theory with both basis sets gave similarly accurate vibrational frequency predictions for monomeric imidazole with a best mean deviation for the DFT/B3LYP/6-31++G** method. The assignment of the matrix spectra of the two isomeric H-bond complex species, N−H···OH_2 and N···H−OH, was performed by comparison with the theoretically predicted IR frequencies and intensities and was further assisted by asymmetrical deuteration experiments. The MP2 and DFT methods employed with the basis set augmented with diffuse functions gave good predictions of the frequency shifts for the vibrational modes directly influenced by the H-bond interaction. For the other vibrational modes, the RHF method performed almost as equally well as the MP2 and DFT methods and we can conclude that this method can provide qualitative and quantitively reliable data on hydrogen-bonded systems.

Introduction

In a former series of reports, we demonstrated that the coupling of matrix-isolation FTIR spectrometry to *ab initio* computational methods can now be considered as one of the most suitable approaches for evaluating intrinsic tautomeric and H-bonding characteristics of polyfunctional bases. This experimental−theoretical approach allowed a detailed description of the tautomeric and H-bonding behavior of cytosines when applied to a series of model molecules with significant increasing tautomeric and H-bonding complexity.[1] Useful correlations between the *ab initio* predicted (water) complex parameters, such as interaction energies and scaling factors for the H-bonded vibrational modes, and experimental parameters, such as frequency shifts and proton affinities, were established, and these may help in the interpretation of experimental vibrational spectra of H-bonded polyfunctional molecules.[2]

The *ab initio* methodology that we have previously used to study rather large H-bonded systems, e.g., 1-CH_3-cytosine·H_2O, involved extended basis sets (6-31++G**), combined with the RHF (restricted hartree fock) method and MP2 (the electron correlation effects accounted for by the second-order perturbation theory), to calculate parameters such as the relative and H-bond energies and vibrational modes. The obtained results have usually agreed very well with the experimentally observed frequencies and frequency shifts when proper scaling factors were applied to the predicted frequency values. Owing to constantly improving computational capabilities and the increasing popularity of density functional theory (DFT) methods, there exists a tendency to leave the relatively fast RHF method behind. In this paper we compare geometry, energy, and vibrational frequency predictions obtained at three levels of theory, RHF, MP2 (MP2 = MBPT2 second-order many-body perturbation theory), and DFT/B3LYP (see Theoretical Method), and two basis sets (6-31G** and 6-31++G**) for monomeric and hydrogen-bonded imidazole (IM), and with the experimental matrix-isolation data. The last two theoretical methods account for the majority of the electron correlation effects, the former in a pure *ab initio* way by treating the electron correlation as a perturbation to the Hartree−Fock Hamiltonian and the latter by using functionals parametrized based on some empirical qualities to account for the exchange and correlation energy contributions.

Recently, a large number of papers have reported on the quality of DFT methods and their ability to predict geometries, harmonic frequencies, and binding energies.[3−13] The B3LYP hybrid method seems to be the best developed so far for this purpose. Rauhut and Pulay demonstrated that the hybrid DFT method is a reliable tool for prediction and interpretation of IR spectra of organic molecules, with the best mean deviation of 18.5 cm^{-1} for vibrations on some selected 31 organic molecules.[8] Recently, Kwiatkowski and Leszczynski reported predicted spectra of the most stable tautomers of cytosine at the RHF/6-31G** and DFT/B3LYP/6-31G** levels of theory and compared them with the matrix-isolated IR spectra.[13] They concluded that both methods provide IR frequencies and intensities with similar quality. Salahub *et al.* demonstrated the need for gradient corrected functionals in the DFT calculations of the H-bonded water dimer and the formamide-water dimer.[3] Del Bene *et al.* tested the B3LYP DFT method for eight different

[†] University of Leuven.
[‡] University of Arizona.
[§] Polish Academy of Sciences.
[||] Senior Research Associate of the Belgian National Fund for Scientific Research.
* To whom correspondence should be addressed.
[⊗] Abstract published in *Advance ACS Abstracts,* March 1, 1997.

S1089-5639(96)03711-5 CCC: $14.00

TABLE 1: Internal Coordinates[a] Used in the Normal Mode Analysis for Imidazole, Imidazole·H_2O $N_4\cdots$HOH Complex, and $N_1H\cdots OH_2$ Complex

(a) Imidazole	
$S_1 = r_{1,2}$	$\nu(N_1C_2)$
$S_2 = r_{2,3}$	$\nu(C_2C_3)$
$S_3 = r_{3,4}$	$\nu(C_3N_4)$
$S_4 = r_{4,5}$	$\nu(N_4C_5)$
$S_5 = r_{5,1}$	$\nu(C_5N_1)$
$S_6 = r_{1,8}$	$\nu(N_1H_8)$
$S_7 = r_{2,6}$	$\nu(C_2H_6)$
$S_8 = r_{3,7}$	$\nu(C_3H_7)$
$S_9 = r_{5,9}$	$\nu(C_5H_9)$
$S_{10} = (2^{-1/2})\,(\delta_{6,1,2} - \delta_{6,3,2})$	$\delta(C_2H_6)$
$S_{11} = (2^{-1/2})\,(\delta_{9,1,5} - \delta_{9,4,5})$	$\delta(C_5H_9)$
$S_{12} = (2^{-1/2})\,(\delta_{7,2,3} - \delta_{7,4,3})$	$\delta(C_3H_7)$
$S_{13} = (2^{-1/2})\,(\delta_{8,5,1} - \delta_{8,2,1})$	$\delta(N_1H_8)$
$S_{14} = \gamma_{8,2,1,5}$	$\gamma(N_1H_8)$
$S_{15} = \gamma_{6,1,2,3}$	$\gamma(C_2H_6)$
$S_{16} = \gamma_{9,4,5,1}$	$\gamma(C_5H_9)$
$S_{17} = \gamma_{7,2,3,4}$	$\gamma(C_3H_7)$
$S_{18} = (2.5^{-1/2})(\delta_{5,2,1} + a\,(\delta_{1,4,5} + \delta_{1,3,2}) + b\,(\delta_{5,3,4} + \delta_{2,4,3}))$[b]	δ_{R1}
$S_{19} = (1/3)((a - b)(\delta_{1,3,2} - \delta_{1,4,5}) + (1 - a)\,(\delta_{5,3,4} - \delta_{2,4,3}))$	δ_{R2}
$S_{20} = (2.5^{-1/2})\,(\tau_{2,3,4,5} + b\,(\tau_{5,1,2,3} + \tau_{2,1,5,4}) + a\,(\tau_{1,2,3,4} + \tau_{1,5,4,3}))$	τ_{R1}
$S_{21} = (1/3)\,((a - b)\,(\tau_{1,2,3,4} - \tau_{1,5,4,3}) + (1 - a)\,(\tau_{5,1,2,3} - \tau_{2,1,5,4}))$	τ_{R2}
(b) Imidazole·H_2O $N_4\cdots$HOH Complex	
$S_{22} = (2^{-1/2})(r_{10,11} + r_{12,11})$	ν^f_{OH}
$S_{23} = (2^{-1/2})(r_{10,11} - r_{12,11})$	ν^b_{OH}
$S_{24} = r_{4,11}$	$\nu_{(N\cdots HO)}$
$S_{25} = \delta_{10,11,12}$	$\delta_{(HOH)}$
$S_{26} = (2^{-1/2})\,(\delta_{10,4,5} - \delta_{10,4,3})$	$\delta_{(N\cdots HO)}$
$S_{27} = (2^{-1/2})\,(\delta_{11,4,5} - \delta_{11,4,3})$	i.p. butterfly
$S_{28} = \gamma_{11,4,5,3}$	o.o.p. butterfly
$S_{29} = \gamma_{10,4,5,3}$	$N\cdots HO$ o.o.p. wag
$S_{30} = (2^{-1/2})\,(\tau_{12,11,4,5} + \tau_{12,11,4,3})$	HO torsion about $N\cdots OH$
(c) $N_1H\cdots OH_2$ Complex	
$S_{22} = (2^{-1/2})\,(r_{11,10} + r_{12,10})$	ν^s_{HOH}
$S_{23} = (2^{-1/2})\,(r_{11,10} - r_{12,10})$	ν^a_{HOH}
$S_{24} = r_{1,10}$	$\nu_{N\cdots HO}$
$S_{25} = \delta_{12,11,10}$	δ_{HOH}
$S_{26} = \delta_{10,1,2}$	o.o.p. butterfly
$S_{27} = \delta_{11,1,2}$	H_2O o.o.p. translation
$S_{28} = \delta_{12,1,10}$	H_2O i.p. wag
$S_{29} = \gamma_{10,1,5}$	i.p. butterfly
$S_{30} = (2^{-1/2})(\tau_{12,10,1,2} + \tau_{11,10,1,2})$	H_2O twist

[a] $r_{i,j}$ indicates stretch of bond $i - j$, $\delta_{i,j,k}$ bend of the angle between the bonds $i - j$ and $j-k$, $\gamma_{i,j,k,l}$ bend of the bond $i - k$ out of the plane defined by the bonds $j - k$ and $i - l$, and $\tau_{i,j,k,l}$ torsion of the plane defined by the bonds $i - j$ and $j - k$ with respect to the plane defined by the bonds $j - k$ and $k - l$, o.o.p. out of plane, i.p in plane. [b] $a = -0.809$; $b = 0.309$. [c] Atom numbering as in Scheme 1.

H-bonded complexes and concluded that the B3LYP/6-31G** method fails to yield reliable binding energies, intermolecular distances, and vibrational frequencies. The use of a larger basis set (6-31+G**) yielded better data, but the MP2/6-31+G** results were still in better agreement with experimental results.[9]

Our studies on IM and its complexes with water are motivated by its occurrence in nucleic acid bases as the 5-ring part of adenine and guanine. In the presence of one water molecule, hydrogen bonding gives rise to two possible complexes where either IM or water acts as the proton donor: $N{-}H\cdots OH_2$ and $N\cdots H{-}OH$. The vibrational spectrum of IM has been studied in the gas phase[14] and in Ar matrices.[15] *Ab initio* studies of IM have been limited to the RHF/3-21G[16] and RHF/4-21G[16,17] levels. The H-bonding between IM and H_2O have been investigated at the RHF and MP2 levels.[18−20] DFT calculations have not yet been performed for IM and their H-bonded complexes.

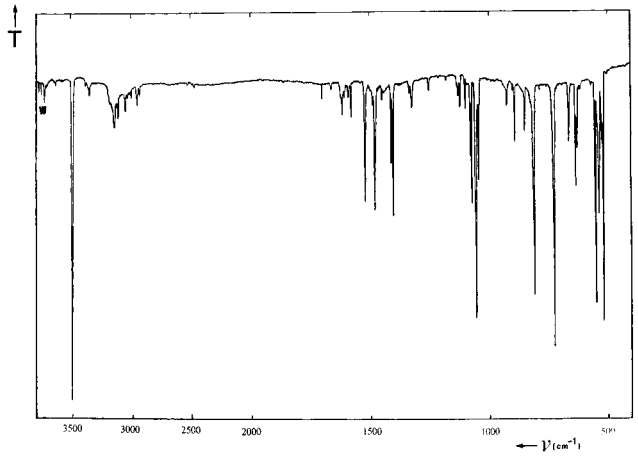

Figure 1. FTIR spectrum of imidazole in Ar at 12 K (w = water impurity).

In this paper we compare results of three different computational methods (RHF, MP2, and DFT/B3LYP) and two basis sets (6-31G** and 6-31++G**) with new experimental data for water complexes of IM isolated in Ar matrices. To our knowledge, this is the first time such a comparison is made for larger H-bonded complexes, employing more extended basis sets and the gradient-corrected functionals in the DFT method. The present results allow us to critically review the accuracy of our previous studies of cytosine model molecules that were made at the SCF/6-31++G** and MP2/6-31++G** levels.[1,2] They also provide an initial theoretical approach that will be needed to assign spectra of an adenine model system, which will be studied next.

Methodology

Experimental Method. The cryogenic (Air Products Displex 202E) and the FTIR (Bruker IFS-88) equipment used in this work have been described in detail previously.[21,22] To evaporate the solid IM into the jet of argon, the homemade minifurnace [22] was installed into the cryostat and the optimal sublimation temperatures were found to be 20 °C at an Ar deposition rate of 5 mmol/h^{-1}. Dimerization of IM in Ar occurs only above sublimation temperatures of 25 °C.[23] IM/H_2O/Ar samples were studied at IM/Ar ratios similar to those applied in the study of the monomeric IM, while the IM/H_2O ratio varied between 1/1 and 1/5. As has been demonstrated before,[1b,21] the latter ratio ensures an excess amount of 1:1 H-bonded complexes IM/H_2O to be present in the Ar matrix with still rather weak spectral manifestations of higher stoichiometry complexes, which are not discussed in this paper.

The compound IM (99%) was commercially available from Janssen Chimica. Although the deuterated compound IM-d_4 was also commercially available (Aldrich Europe), the extent of deuteration appeared to be only about 70%. However, this was sufficient for the purpose of discrimination between the two complexes considered in this work. Twice-distilled water was used for the experiments with water-doped samples, while Ar gas of the highest purity available (99.9999%) from Air Liquide was used in all experiments.

Theoretical Method. Three different computational methods were used in this work, and for all three of them the 6-31++G** and 6-31G** basis sets were employed for the molecular orbital expansion. First, we considered the Hartree−Fock method. The RHF/6-31++G** level of theory has been demonstrated in our previous studies to produce quite accurate results for isolated

TABLE 2: RHF, DFT/B3LYP, and MP2 Predicted Geometry Parameters of Imidazole and the H-Bonded Complexes with Water Using the 6-31++G and the 6-31G** Basis Sets**

		free				N_1—H···OH_2			N_4···HO—H		
		RHF	MP2	DFT	expt[32]	RHF	MP2	DFT	RHF	MP2	DFT
						Distances (Å)					
N_1—C_2	*a*	1.372	1.377	1.381	1.377	1.369	1.375	1.379	1.373	1.377	1.382
	b	1.372	1.375	1.380	1.369	1.373	1.377	1.372	1.375	1.381	
C_2—C_3	*a*	1.353	1.380	1.375	1.364	1.355	1.381	1.376	1.352	1.379	1.373
	b	1.351	1.377	1.372	1.352	1.379	1.374	1.349	1.377	1.371	
C_3—N_4	*a*	1.371	1.378	1.379	1.382	1.370	1.378	1.378	1.372	1.378	1.379
	b	1.371	1.376	1.378	1.370	1.375	1.378	1.372	1.376	1.378	
N_4—C_5	*a*	1.291	1.327	1.316	1.314	1.294	1.330	1.319	1.293	1.329	1.318
	b	1.289	1.324	1.315	1.292	1.328	1.318	1.292	1.327	1.318	
C_5—N_1	*a*	1.350	1.368	1.368	1.364	1.347	1.365	1.366	1.347	1.364	1.364
	b	1.350	1.366	1.367	1.346	1.363	1.364	1.345	1.362	1.362	
N_1—H	*a*	0.993	1.008	1.009	0.998	0.998	1.015	1.016	0.993	1.009	1.009
	b	0.992	1.007	1.008	0.998	1.016	1.019	0.992	1.007	1.008	
C_2—H	*a*	1.069	1.076	1.079	1.079	1.069	1.076	1.079	1.068	1.076	1.079
	b	1.069	1.075	1.079	1.069	1.075	1.079	1.068	1.075	1.079	
C_3—H	*a*	1.070	1.078	1.081	1.078	1.070	1.077	1.081	1.069	1.077	1.080
	b	1.070	1.077	1.081	1.070	1.077	1.082	1.070	1.076	1.080	
C_5—H	*a*	1.071	1.078	1.081	1.079	1.071	1.077	1.081	1.071	1.077	1.081
	b	1.071	1.077	1.081	1.071	1.078	1.082	1.071	1.076	1.080	
H···O or H···N	*a*	2.063	1.938	1.955	2.089	1.945	1.928				
	b	2.032	1.922	1.913	2.109	2.006	1.981				
N···O	*a*	3.061	2.953	2.972	3.031	2.915	2.904				
	b	3.030	2.938	2.932	2.971	2.881	2.860				
O—H (water)	*a*	0.943	0.963	0.965	0.96	0.944	0.965	0.965	0.951[c]	0.977[c]	0.981[c]
		0.943	0.963	0.965	0.944	0.965	0.965	0.942[d]	0.963[d]	0.964[d]	
	b	0.943	0.961	0.965	0.96	0.943	0.962	0.965	0.950[c]	0.972[c]	0.976[c]
		0.943	0.961	0.965	0.943	0.962	0.965	0.943[d]	0.962[d]	0.965[d]	
						Angles (deg)					
$N_1C_2C_3$	*a*	105.23	104.96	105.07	105.48	105.47	105.30	105.40	105.31	105.11	105.21
	b	105.16	104.89	105.02	105.51	105.27	105.43	105.30	105.02	105.17	
$C_2C_3N_4$	*a*	110.35	110.85	110.66	110.69	110.24	110.75	110.53	110.08	110.41	110.22
	b	110.50	111.05	110.84	110.34	110.94	110.72	110.17	110.55	110.34	
$C_3N_4C_5$	*a*	105.47	105.07	105.43	104.93	105.24	104.79	105.12	105.73	105.61	105.91
	b	105.32	104.87	105.18	105.05	104.51	104.80	105.63	105.46	105.74	
$H_8N_1C_2$	*a*	126.78	126.19	126.32	126.90	126.98	126.50	126.62	126.14	126.27	
	b	126.76	126.12	126.28		127.00	126.49	126.67	126.76	126.07	126.26
HOH (water)	*a*	107.09	105.36	105.74	104.5	107.41	106.04	106.51	106.70	105.02	105.62
	b	105.99	103.83	103.75		106.89	104.89	105.00	105.43	103.03	106.38

[a] 6-31++G** basis set. [b] 6-31G** basis set. [c] H-bonded H atom. [d] Free H atom.

SCHEME 1

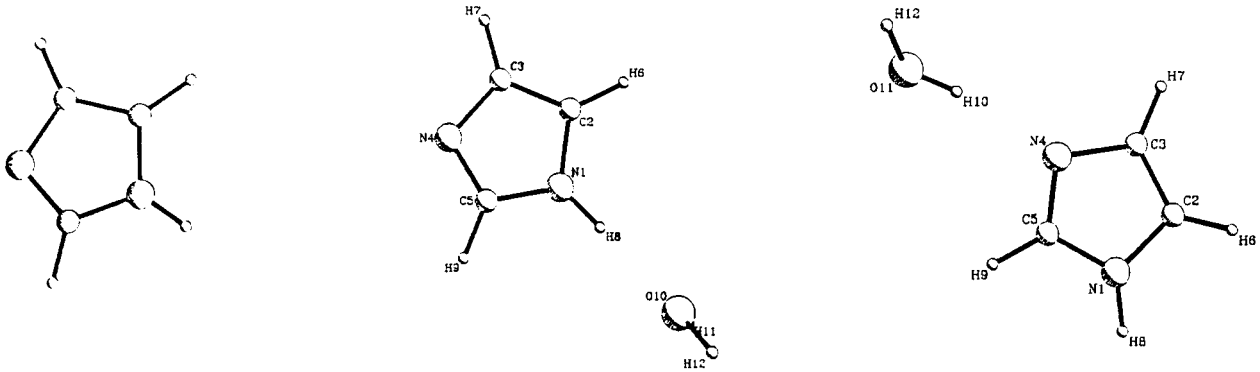

molecules of nucleic bases and some model molecules.[1,2] The comparison of the two basis sets allows us to estimate the importance of the diffuse functions.

The HF energy is given as

$$E_{HF} = E_T + E_V + E_J + E_X$$

where E_T is the kinetic energy, E_V the potential energy involving the nuclei, and E_J and E_X are the Coulomb and exchange parts of the electron−electron repulsion energy.[24] The RHF method was used in the present mode for optimizations of molecular structures, which were followed by single-point MP2 calculations with the same basis set. The MP2 energy obtained for the RHF optimized molecular structure will be denoted as MP2//RHF.

The choice of the basis set was based on the consideration that in order to accurately represent the electronic structure of the monomers with special emphasis on the peripheral regions of the wave functions, which are important for weak intermolecular bonding effects, it is essential to employ sets of orbitals that possess sufficient diffuseness and angular flexibility.[25] To account for electron correlation in the optimization of monomeric IM, we used the second-order many-body perturbation method (MBPT2 or MP2) and the density functional theory

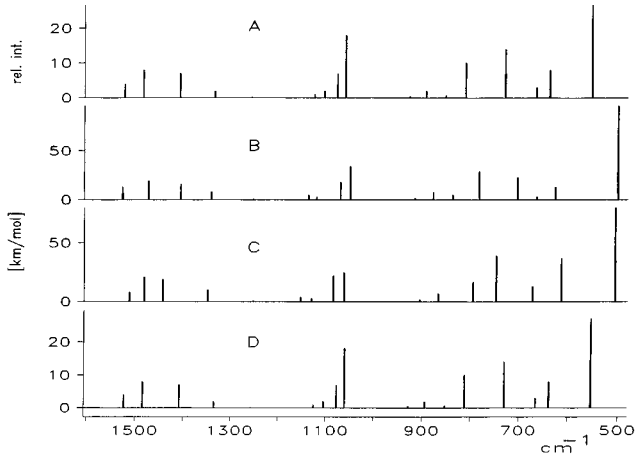

Figure 2. Comparison between the experimental spectrum of imidazole in Ar (12 K) (A) and the spectra predicted at DFT/B3LYP (B), MP2 (C), and RHF (D) levels using the 6-31G** basis set (only the main band of the experimental multiplets are shown in (A)).

(DFT) method with the hybrid of Becke's nonlocal three-parameter exchange and correlated functional with the Lee−Yang−Parr correlation functional.[26,27] The DFT energy is given as

$$E_{\mathrm{DFT}} = E_{\mathrm{HF}} - E_{\mathrm{X}} + E_{\mathrm{XC}}$$

where E_{XC} is defined by the following exchange correlation functional:

$$E_{\mathrm{XC}} = a_0 E_{\mathrm{X}}^{\mathrm{UEG}} + (1 - a_0) E_{\mathrm{X}}^{\mathrm{HF}} + a_{\mathrm{x}} \Delta E_{\mathrm{x}} + E_{\mathrm{c}}^{\mathrm{UEG}} + a_{\mathrm{c}} \Delta E_{\mathrm{c}}$$

wherein $E_{\mathrm{X}}^{\mathrm{UEG}}$ and $E_{\mathrm{C}}^{\mathrm{UEG}}$ are the density functionals for the exchange and correlation in the uniform electron gas, $E_{\mathrm{X}}^{\mathrm{HF}}$ the Hartree−Fock exchange energy, and the ΔE terms are the nonlocal exchange- and correlation-type gradient corrections. The coefficients used in the formula are the ones from Becke, $a_0 = 0.80$, $a_{\mathrm{x}} = 0.72$, and $a_{\mathrm{c}} = 0.81$, determined from a best fitting of the heats of formation of a representative set of molecules.[26] The integration grid used in the DFT method was the so-called fine grid of the GAUSSIAN package, which consists of 75 radial shells and 302 angular points for every atom.

The total energy was corrected for the zero-point vibrational energy calculated with single scaling factors (0.90 for RHF, 0.96 for MP2, and 0.97 for DFT). The IR frequencies and intensities were computed analytically, for RHF and DFT, and numerically, for MP2, by the standard procedures incorporated in the programs GAUSSIAN 92 and GAUSSIAN 94.[28]

In order to express normal coordinates in terms of a molecule-fixed coordinate system, internal coordinates were defined for the monomers and symmetry coordinates were expressed in terms of these internal coordinates. Table 1 lists internal and symmetry coordinates for IM. The potential energy distribution (PED) of the vibrational modes over the internal coordinates was calculated using the following steps. First, linear transformation matrices were found for the Cartesian, normal, and internal coordinates. Next, the Cartesian force constant matrix was transformed into the force constant matrix expressed in the internal coordinates. The basis for the PED matrix elements was then calculated with the following expression:

$$\lambda_i = \sum_{\rho\sigma}^{3N-6} L_{\rho i} F_{\rho\sigma} L_{\sigma i}$$

where L is the linear transformation matrix between the internal and normal coordinates and F the force constant matrix in the internal coordinates.[29]

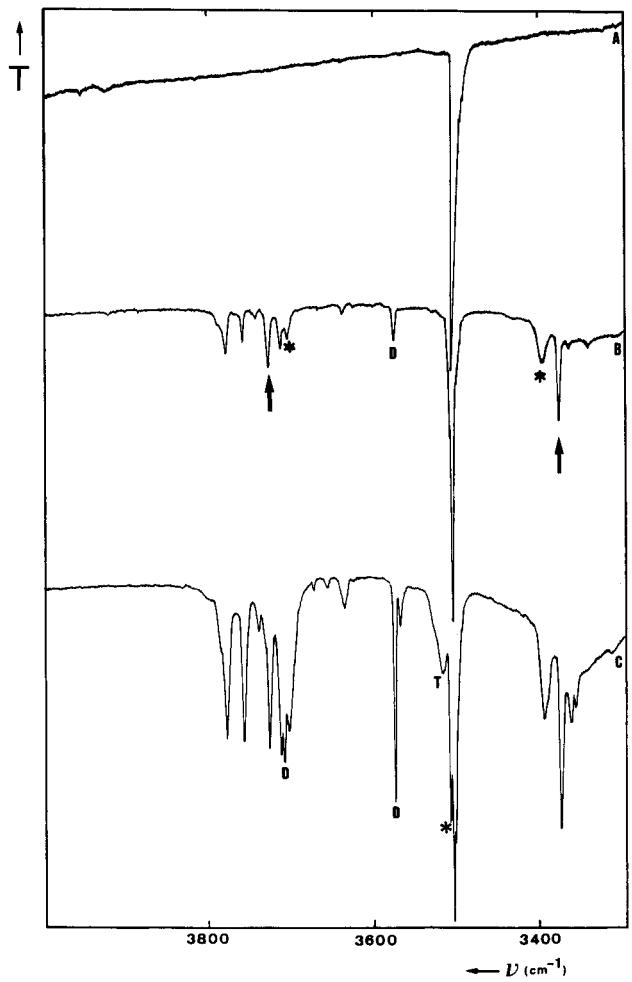

Figure 3. $\nu_3 - \nu_1(H_2O)$ and ν_{NH} region of the FTIR spectrum of imidazole/Ar (A) and imidazole/H_2O/Ar (B, C) at 12 K: (B) H_2O/Ar = 1/1000; (C) H_2O/Ar = 1/500; ↑ = N−H···OH_2 complex; * = N···HO−H complex; D, T = water dimer, trimer).

The $PED_{i\rho}$ PED-matrix element $PED_{i\rho} = \sum_{\sigma}^{3N-6} L_{\rho i} F_{\rho\sigma} L_{\sigma i}/\lambda_i$ represents the contribution usually expressed of the molecular vibration along the ρth internal coordinate to the molecular vibration along the ith normal coordinate.

In the calculations for the H-bonded complexes with H_2O, a similar approach was followed as described above.

In the case of the bonded water modes that are characterized by larger anharmonicities, the formerly developed anharmonicity correction procedure[1,2] was applied in order to compare the predicted frequencies and frequency shifts with their experimental analogues. The total energy of the complexes was computed as for the IM monomer, but the results were corrected for the basis set superposition error (BSSE) by recalculating the monomer energies in the basis set of the hetero-dimers using the so-called counterpoise method.[30,31]

The BSSE corrected interaction energy is then calculated as

$$\Delta E_{\mathrm{A}\cdots\mathrm{B}} = E_{\mathrm{A}\cdots\mathrm{B}} - E_{\mathrm{A(B)}} - E_{\mathrm{B(A)}}$$

where $E_{\mathrm{A}\cdots\mathrm{B}}$ is the energy of the H-bonded complex, E_{A} the energy of the monomer A obtained with the extra ghost Gaussian functions placed at the positions of the nuclei of B, and E_{B} the energy of monomer B obtained with the extra ghost functions placed at the positions of the nuclei of A.

Results and Discussion

Monomer Compound in Ar. All three levels of theory yield bond distances and bond angles quite close to the experimental

TABLE 3: Experimental (Ar Matrix) and Calculated (RHF, MP2, or DFT/6-31++G) Vibrational Data for Imidazole (in a Band Pair the Most Intense Absorption Is Italicized)**

exptl		calcd ν (cm^{-1})			exptl I (km/mol)			calcd I (km/mol						
ν (cm^{-1})	ref 15 (cm^{-1})	RHF[a]	MP2[b]	DFT[c]	RHF[d]	MP2[e]	DFT[f]	RHF	MP2	DFT	PED[g]	RHF	MP2	DFT
3500	3504	3535	3575	3558	103	77	57	103	77	57	$\nu(N_1H)$	99	100	100
		3496	3463	3484										
3114?		3113	3226	3192	<1	<1	<1	2	<1	1	$\nu(C_2H)$	79	78	86
			3125	3126							$\nu(C_3H)$	30	20	13
		3087	3202	3164	<1	<1	<1	1	3	5	$\nu(C_5H)$	25		
			3102	3099							$\nu(C_3H)$	57	79	84
											$\nu(C_2H)$	18	20	12
3090?		3086	3208	3164				7	<1	1	$\nu(C_3H)$	22		
			3108	3102							$\nu(C_5H)$	74	97	95
1524/*1522*	1518	1557	1498	1516	8	7	4	25	6	12	$\nu(C_2C_3)$	26	40	33
				1524							$\delta(N_1H)$	13	18	16
											$\nu(N_4C_5)$	36	14	13
											$\delta(C_3H)$	12	13	13
1483	1480	1487	1464	1461	14	11	8	29	27	23	$\nu(N_4C_5)$	15	26	20
				1468							$\delta(C_5H)$	17	26	21
											$\nu(C_5N_1)$	12	14	11
											$\delta(C_2H)$	21	16	
											$\nu(C_2C_3)$	26		30
1415/*1407*	1404	1420	1427	1395	13	10	7	26	19	16	$\nu(N_1C_2)$	12	28	17
				1402							$\delta(N_1H)$	43	27	38
											$\nu(C_5N_1)$	20	21	21
											$\nu(C_2C_3)$	12		10
1339/*1333*	1325	1347	1339	1333	3	2	2	10	8	7	$\nu(N_4C_5)$	32	25	31
				1340							$\delta(C_3H)$	22	25	23
											$\nu(C_3N_4)$	16	23	19
											$\nu(C_2C_3)$	13		10
1256	1252	1264	1245	1247	<1	<1	<1	<1	1	<1	$\delta(C_5H)$	49	47	49
				1254							$\delta(C_3H)$	21	21	21
											$\nu(N_4C_5)$	11	17	12
											$\delta(C_2H)$	11		10
1132/*1124*	1130	1108	1143	1132	4	2	1	5	3	4	$\nu(C_3N_4)$	58	53	60
				1138							$\nu(N_1C_2)$	19	29	24
1106/*1103*	1120	1125	1122	1116	2	3	2	6	4	4	$\nu(C_5N_1)$	29	33	23
				1121							$\delta(C_2H)$	19	14	16
											$\nu(C_2C_3)$	17	12	11
											$\delta(C_3H)$	16	11	12
											$\delta(N_1H)$		18	14
											$\delta(C_5H)$		11	12
1082/*1076*	1074	1065	1077	1066	12	9	7	16	26	23	$\delta(N_1H)$	18	22	25
				1072							$\delta(C_3H)$	16	23	18
											$\nu(C_2C_3)$	14	16	13
											$\nu(N_1C_2)$		14	14
											$\nu(C_5N_1)$	29		18
1059/1048	1056	1037	1054	1045	33	25	18	60	30	40	$\delta(C_2H)$	21	34	31
				1050							$\nu(N_1C_2)$	47	17	26
											$\nu(C_5N_1)$		14	12
927	916	913	901	912	<1	<1	<1	2	2	2	δ_{R1}	85	87	85
				917										
902/*893*	892	884	863	877	1	2	2	6	5	6	δ_{R2}	88	87	87
			783	881							$\gamma(C_2H)$			14
852	850	899	751	841	2	<1	<	<1	55	7	$\gamma(C_3H)$	65	104	94
			783	850							$\gamma(C_5H)$	23		
											$\gamma(C_2H)$	21		14
811	810	870	710	784	19	14	10	25	42	42	$\gamma(C_5H)$	80	95	97
			739	792							$\gamma(C_3H)$	24		
											$\gamma(C_2H)$		12	
735/*729*	735/728	752	645	702	36	27	14	69	8	41	$\gamma(C_3H)$	82	37	89
											$\gamma(C_3H)$	16		τ_{R2}
												51		
664	662	654	631	656	5	3	3	13	3	5	τ_{R1}	16	52	26 τ_{R2}
			658	663								84		77 $\gamma(C_2H)$
												37		
637/634/630	636/631	618	576	620	14	10	8	7	44	13	τ_{R2}	25	52	33
											τ_{R1}	77	25	67
											$\gamma(C_2H)$		13	
											$\gamma(N_1H)$		13	
553/540/*522*	551/538	497	432	502	49	37	27	133	60	96	$\gamma(N_1H)$	92	78	89 τ_{R1}
			450	507								23		

[a] First row: uniform scaling factor 0.90; second row: scaling factor 0.89 for ν(NH). [b] First row: uniform scaling factor 0.96; second row: scaling factor 0.93 for ν(XH), and 1.00 for γ and τ. [c] First row: uniform scaling factor 0.97; second row: scaling factor 0.95 for ν(XH), 0.98 for γ and τ, and 0.975 for other. [d] Experimental intensities normalized to the RHF-calculated value for $\nu(N_1H)$ (103 km mol^{-1}) [e] Experimental intensities normalized to the MP2-calculated value for $\nu(N_1H)$ (77 km mol^{-1}). [f] Experimental intensities normalized to the DFT-calculated value for $\nu(N_1H)$ (57 km mol^{-1}). [g] PED for calculations performed at RHF, MP2, and DFT levels. Only contributions greater than 10 are listed. PED's are only relevant for the uniformly scaled frequencies.

TABLE 4: Experimental (Ar Matrix) and Calculated (RHF, MP2, or DFT/6-31G) Vibrational Data for Imidazole (in a Band Pair the Most Intense Absorption Is Italicized)**

exptl		calcd ν (cm^{-1})			exptl I (km/mol)			calcd I (km/mol						
ν (cm^{-1})	ref 15 (cm^{-1})	RHF[a]	MP2[b]	DFT[c]	RHF[d]	MP2[e]	DFT[f]	RHF	MP2	DFT	PED[g]	RHF	MP2	DFT
3500	3504	3538	3590	3560	94	505	48	94	71	48	$\nu(N_1H)$	100	100	100
		3499	3478	3487										
3114		3110	3232	3191	<1	<1	<1	4	1	2	$\nu(C_2H)$	81	84	89
			3131	3126							$\nu(C_3H)$	17	14	10
		3082	3203	3160				3	5	8	$\nu(C_3H)$	75	80	82
			3103	3097							$\nu(C_2H)$	18	12	
3090		3079	3207	3162	<1	<1	<1	9	<1	7	$\nu(C_5H)$	92	91	90
			3107	3126										
1524/*1522*	1518	1569	1511	1526	7	6	3	26	8	13	$\nu(C_2C_3)$	27	41	35
											$\delta(N_1H)$	12	17	15
											$\nu(N_4C_5)$	36	14	25
				1534							$\delta(C_3H)$	12	14	13
1483	1480	1498	1480	1472	13	10	7	27	21	19	$\nu(N_4C_5)$	16	26	21
				1480							$\delta(C_5H)$	17	25	21
											$\nu(C_5N_1)$	12	17	11
											$\delta(C_2H)$	21	15	
											$\nu(C_2C_3)$	27		19
1415/*1407*	1404	1427	1442	1405	12	9	6	26	19	16	$\nu(N_1C_2)$	13	31	19
				1411							$\delta(N_1H)$	44	27	37
											$\nu(C_5N_1)$	21		22
											$\nu(C_2C_3)$	11		
1339/*1333*	1325	1354	1347	1347	3	2	2	10	10	8	$\nu(N_4C_5)$	31	25	31
											$\delta(C_3H)$	22	23	23
											$\nu(C_3N_4)$	16	23	19
											$\nu(C_2C_3)$	11		
1256	1252	1267	1252	1252	<1	<1	<1	1	1	1	$\delta(C_5H)$	49	46	49
				1259							$\delta(C_3H)$	21	20	21
											$\nu(N_4C_5)$	11	18	13
											$\delta(C_2H)$	11		10
											$\nu(N_1C_2)$	13		
1132/*1124*	1130	1109	1152	1136	2	3	2	5	3	3	$\nu(C_5N_1)$	24	31	20
				1142							$\delta(C_2H)$	19	14	15
											$\nu(C_2C_3)$	16	11	11
											$\delta(C_3H)$	12	12	21
											$\delta(N_1H)$		18	14
											$\delta(C_5H)$		12	12
1106/*1103*	1120	1128	1129	1119	3	2	1	4	4	5	$\nu(C_3N_4)$	59	53	59
				1125							$\nu(N_1C_2)$	19	29	52
1082/*1076*	1074	1068	1083	1069	11	8	6	13	22	18	$\delta(N_1H)$	19	24	27
				1074							$\delta(C_3H)$	16	23	17
											$\nu(C_2C_3)$	13	15	13
											$\nu(N_1C_2)$		13	13
											$\nu(C_5N_1)$	30		20
1059/1048	1056	1040	1061	1049	30	23	15	57	25	34	$\delta(C_2H)$	22	35	31
				1054							$\nu(N_1C_2)$	47	16	26
											$\nu(C_5N_1)$		13	11
927	916	918	904	915	<1	<1	<1	2	2	2	δ_{R1}	85	88	86
				919										
902/*893*	892	886	866	877	2	<1	<1	7	7	8	δ_{R2}	88	88	87
				881										
852	850	903	794	837	1	2	1	<1	17	5	$\gamma(C_3H)$	65	106	95
			827	846							$\gamma(C_5H)$	23		
											$\gamma(C_2H)$	21		13
811	810	872	746	782	17	13	8	15	39	29	$\gamma(C_5H)$	80	98	95
			777	790							$\gamma(C_3H)$	25		
735/*729*	735/728	758	671	703	33	25	12	45	13	23	$\gamma(C_2H)$	83	87	89
			699	711							$\gamma(C_3H)$	16		
664	662	660	657	663	5	3	3	12	<1	3	τ_{R1}	21	50	30
			671	669							τ_{R2}	83	48	75
637/634/630	636/631	623	612	625	13	9	3	7	37	13	τ_{R2}	26	34	37
			622	632							τ_{R1}	78	58	66
											$\gamma(N_1H)$		14	
553/540/*522*	551/538	492	505	500	45	34	23	140	80	96	$\gamma(N_1H)$	94	77	90
			526	505							τ_{R1}		26	12

[a] First row: uniform scaling factor 0.90; second row: scaling factor 0.89 for ν(NH). [b] First row: uniform scaling factor 0.96; second row: scaling factor 0.93 for ν(XH), and 1.00 for γ and τ. [c] First row: uniform scaling factor 0.97; second row: scaling factor 0.95 for ν(XH), 0.98 for γ and τ, and 0.975 for other. [d] Experimental intensities normalized to the RHF-calculated value for $\nu(N_1H)$ (94 km mol^{-1}). [e] Experimental intensities normalized to the MP2-calculated value for $\nu(N_1H)$ (71 km mol^{-1}). [f] Experimental intensities normalized to the DFT-calculated value for $\nu(N_1H)$ (48 km mol^{-1}). [g] PED for calculations performed at RHF, MP2, and DFT levels. Only contributions greater than 10 are listed. PED's are only relevant for the uniformly scaled frequencies.

gas phase values (Table 2),[32] although the best results are obtained by the correlated MP2 and DFT methods. The RHF method predicts bond lengths that are too short compared to the predictions of MP2 and DFT. The FTIR spectrum of IM

TABLE 5: (A) *Ab Initio* Calculated Energy Components (au), Relative Energies (kJ/mol), and Dipole Moments (D) for Imidazole and Its Two 1:1 H-Bonded Complexes with H_2O and (B) Basis Set Superposition Error Corrected Interaction Energies[d]

			imidazole···H_2O	
		imidazole	N_1—H···OH_2	N_4···H—OH
		(A)		
RHF (au)	*a*	−224.832 787 9	−300.873 522 9	−303.874 112 9
	b	−224.824 299 1	−301.858 030 2	−300.859 016 9
MP2[a] (au)	*a*	−225.565 985 4	−301.810 985 5	−301.811 535 1
	b	−225.549 869 9	−301.781 578 1	−301.783 334 7
ZPE[b] (au)	*a*	0.069 074 2	0.091 851 2	0.092 484 9
	b	0.069 206 84	0.091 868 4	0.093 041 1
total (au) RHF	*a*	−224.763 713 7	−300.781 671 7	−300.781 628 0
	b	−224.755 092 7	−300.766 161 8	−300.765 975 8
MP2	*a*	−225.496 911 0	−301.719 134 3	−301.719 050 2
	b	−225.480 663 5	−301.689 709 7	−301.690 2936
ΔE[c] (kJ/mol) RHF	*a*		0.00	0.11
	b		0.00	0.49
MP2	*a*		0.00	0.22
	b		1.53	0.00
μ (D)	*a*	3.96	6.78	5.58
	b	3.86	6.75	4.59
		(B)		
RHF + ZPE (complex) (au)	*a*		−300.781 671 7	−300.781 628 0
MP2 + ZPE (complex)	*a*		−301.719 134 3	−301.719 050 2
RHF (base with ghost water orbitals)	*a*		−224.832 950 0	−224.833 083 3
MP2 (base with ghost water orbitals)	*a*		−225.566 569 9	−225.566 932 7
RHF (water with ghost base orbitals)	*a*		−76.031 783 6	−76.031 721 6
MP2 (water with ghost base orbitals)	*b*		−76.234 165 8	−76.233 688 7
H−bond energy (+ ZPE) (kJ/mol)				
RHF	*a*		−19.56	−19.44
	b		−21.91	−21.42
MP2	*a*		−27.52	−27.30
	b		−29.99	−28.61
ref 20 (6-311++G**/MP2 + ZPE)			−26.92	−23.31
H-bond energy (BSSE + ZPE) RHF	*a*		−17.89	−17.58
MP2	*a*		−21.72	−21.80
ref 20 (6-31G*/MP2/BSSE + ZPE)			−23.65	−17.08

[a] Only valence correlation is considered. [b] Calculated as $0.9 \sum h\nu_i/2$ with ν_i the frequencies at the RHF level. [c] Energy difference between the two H-bonded complexes of imidazole. [d] All calculations were performed with molecular structures optimized at RHF/6-31++G** (a) or RHF/6-31G** (b) level.

TABLE 6: (A) *Ab Initio* Calculated Energy Components (au), Relative Energies (kJ/mol), Interaction Energies (kJ/mol), and Dipole Moments (D) for 1:1 H-Bonded Complexes of Imidazole with H_2O and (B) Basis Set Superposition Error Corrected Interaction Energies[a]

			imidazole···H_2O	
		imidazole	N_1—H···OH_2	N_4···H—OH
		(A)		
MP2 (au)	a	−225.568 830 6	−301.814 946 6	−301.815 676 5
	b	−225.552 517 5	−301.785 433 9	−301.787 183 9
DFT	a	−226.235 509 0	−302.680 105 5	−302.681 758 4
	b	−226.223 096 0	−302.655 698 0	−302.657 169 5
MP2 + ZPE (au)	a	0.068 549 76	0.091 534 8	0.092 279 3
	b	0.069 368 83	0.092 632 8	0.093 723 8
DFT + ZPE	a	0.068 999 01	0.091 676 6	0.092 503 1
	b	0.069 124 14	0.092 229 5	0.093 328 5
total (au) MP2	a	−225.500 280 8	−301.723 411 8	−301.723 397 2
	b	−225.483 148 7	−301.692 801 1	−301.693 460 1
DFT	a	−226.166 510 0	−302.588 428 9	−302.589 255 3
	b	−226.153 971 9	−302.563 468 5	−302.563 8410
μ(D) MP2	a	4.03	6.92	5.75
	b	3.87	6.29	4.75
DFT	a	3.87	6.73	5.94
	b	3.70	6.03	4.73
ΔE (kJ/mol) MP2	a		0.00	0.04
	b		1.73	0.00
DFT	a		2.17	0.00
	b		0.98	0.00
		(B)		
MP2 (with ghost imidazole functions)	a		−76.235 040 8	−76.235 382 3
DFT (with ghost imidazole functions)	a		−76.434 803 9	−76.434 768 8
MP2 (with ghost water functions)	a		−225.569 528 2	−225.569 183 0
DFT (with ghost water functions)	a		−226.235 669 2	−226.235 747 2
interaction energy (kJ/mol) MP2	a		−26.61	−26.57
	b		−28.55	−30.27
DFT	a		−22.13	−24.30
	b		−27.51	−28.49
interaction energy (BSSE corrected)			−21.41	−23.10
MP2	a			
DFT	b		−19.37	−21.42

[a] All calculations were performed with molecular structures optimized at the MP2 or DFT 6-31++G** (a) or 6-31G** (b) level.

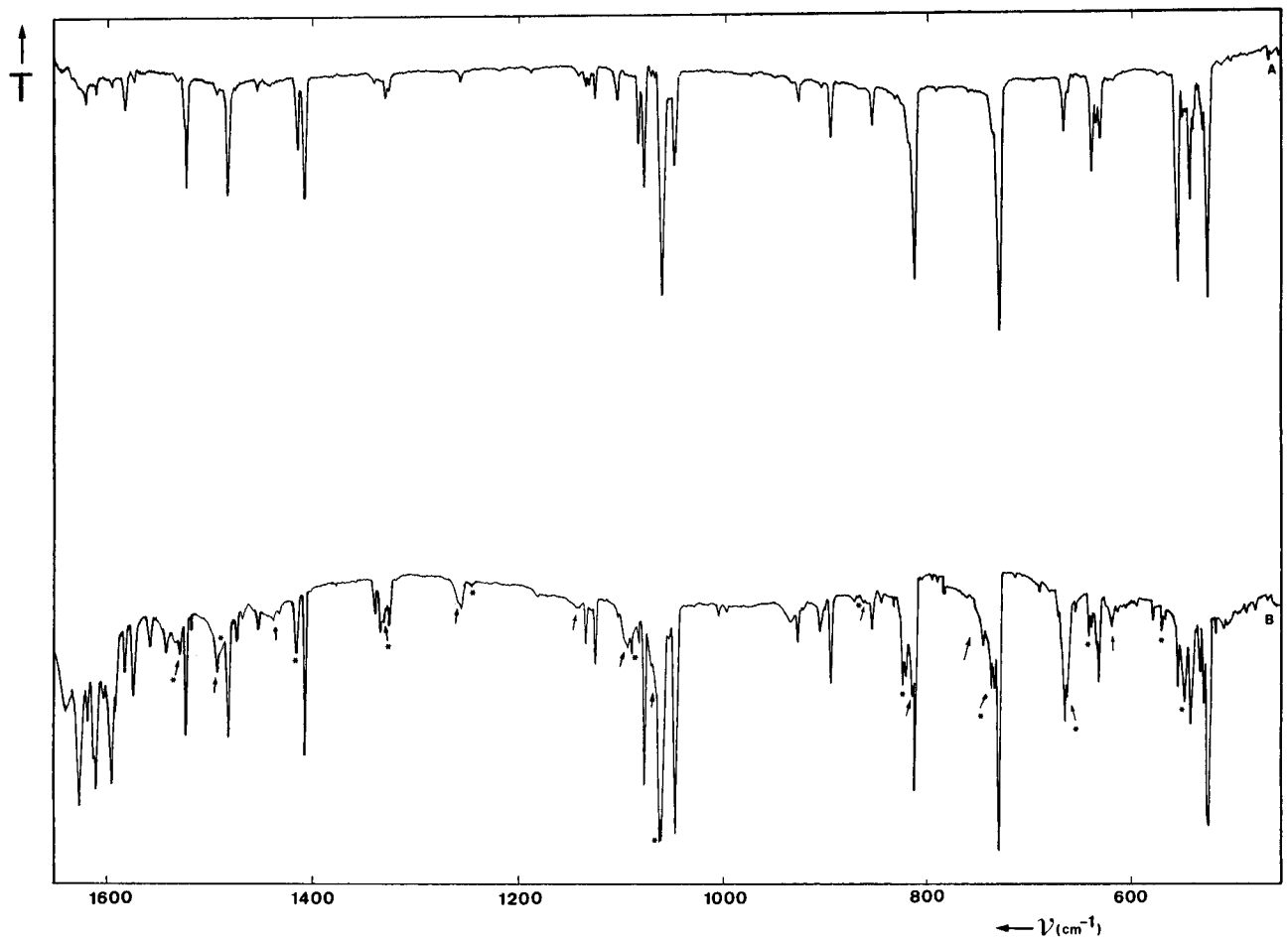

Figure 4. Fingerprint region of the FTIR spectrum of imidazole/Ar (A) and imidazole/H_2O/Ar ((B) H_2O/Ar = 1/500) at 12 K: ↑ = N—H···OH_2 complex; * = N···H—OH complex.

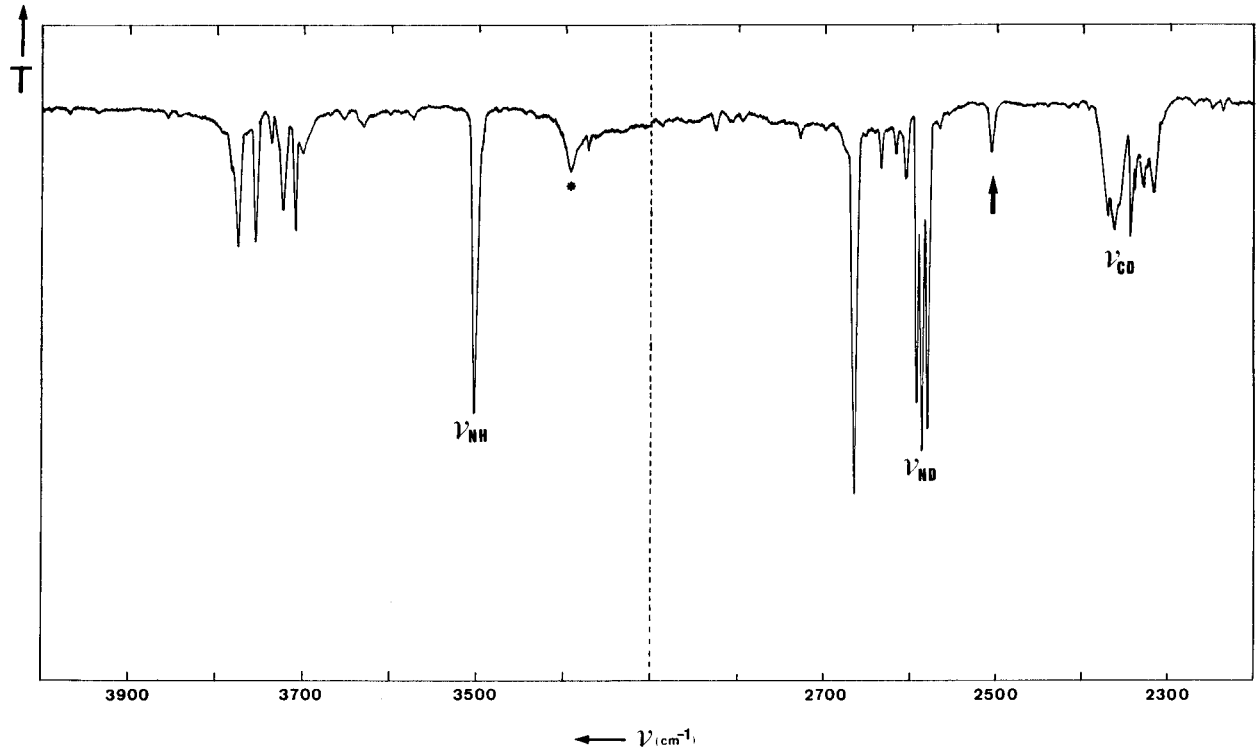

Figure 5. $\nu_3 - \nu_1(H_2O)/\nu_{NH}$ (left) and ν_{ND} (right) spectral regions of the FTIR spectrum of imidazole-d_4 (70%)/H_2O/Ar at 12 K: (H_2O/Ar = 1/2000; ↑ = N—D···OH_2 complex; * = N···HO—H complex).

isolated in Ar is shown in Figure 1. IM (C_s symmetry, Scheme 1) has 21 vibrational modes; 15 involve in-plane molecular distortions (A′) and 6 involve out-of-plane distortions (A″).

The vibrational analysis is summarized in Tables 3 and 4, which compare experimental frequencies and intensities with predicted values obtained at the three different levels of theory

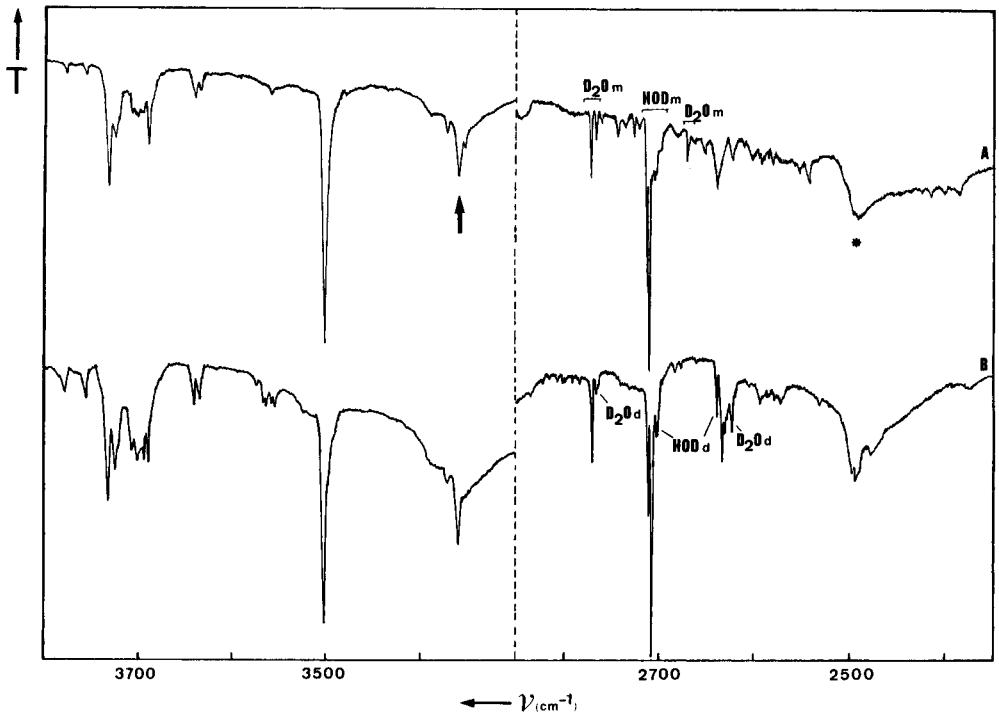

Figure 6. $\nu_3 - \nu_1(H_2O)/\nu_{NH}$ (left) and $\nu_3 - \nu_1(D_2O/HOD)$ region of the FTIR spectrum of imidazole/$D_2O \rightarrow$ HOD $\rightarrow$ H_2O/Ar (D_2O/Ar = 1/500): (A) before annealing; (B) after annealing at 38 K; ↑ = N—H···O complex; * = N···DO complex.

TABLE 7: Estimation of the Relative Concentrations of the N_1—H···OH_2 and N_4···H—OH Complexes of Imidazole Using the Integrated Experimental Intensities (*I*) and the Predicted Intensities (a) at Different Levels of Theory Using the 6-31++G (a) or the 6-31G** (b) Basis Set**

method		*I*(3373)/ *I*(3394)	$a(\nu^{b}_{OH})/a(\nu_{N-H}\cdots)$	[N_1—H···OH_2] [N_4···H—OH]
RHF	a	0.8	1.05	0.84
	b	0.8	0.55	0.44
DFT	a	0.8	1.62	1.30
	b	0.8	0.48	0.38
MP2	a	0.8	1.29	1.03
	b	0.8	0.60	0.48

as well as with those of the earlier matrix study.[15] It must be mentioned that a very small amount of water impurities are manifested in the spectrum shown in Figure 1 (3800−3700 cm^{-1}). However, no trace of dimeric species can be observed in this spectrum.

At least seven experimental absorptions exhibit band splitting, which suggests that the IM molecules can appear in distinct orientations in the matrix. IM modes that are expected to be H-bonding sensitive are not only NH modes, which are easily assigned by comparison with the *ab initio* predictions, but also ring stretches with considerable C_3N_4 and N_4C_5 contributions. The out-of-plane mode γ_{NH} is not a pure group mode in this compound, although the large γ_{NH} PED contribution to the experimental absorption band below 600 cm^{-1} allows this feature to be used for identification of H-bonding interactions.

It is well-known, and also demonstrated in Table 2, that RHF geometry optimization yields bond distances too short when compared to experimental values. Owing to the bond-distance dependence on the static electron correlation, the RHF potential energy surface, which does not include electron correlation contributions, is more sharply curved around the equilibrium geometry than are experimentally fitted potentials. Scaling factors are used to reduce the subsequent error in the vibrational frequencies. Additionally, contributions from vibrational anharmonicity may also become significant in vibrational modes with large amplitude. Single scaling factors of 0.89 or 0.90 for RHF frequencies are most often used. In previous studies, lower scaling factors had to be used for vibrational modes with larger anharmonicity such as ν_{OH} (0.863) and ν_{NH} (0.890).[33] However, the success of the single scaling factor method for RHF-predicted frequencies indicates that the sum of the errors originating from vibrational anharmonicity and from the internuclear distance dependence on electron correlation energy is more or less constant.[34] The cancellation of errors, however, can be totally different for the correlated methods.

When a single scaling factor is used, the mean frequency deviation $|\nu^{exp} - \nu^{th}|$ is 17 cm^{-1} at the RHF level, 41 cm^{-1} at the MP2 level, and 23 cm^{-1} at the DFT level of theory for the 6-31++G** basis set calculations. The modes that particularly deviate from the experimental frequencies are the ν_{XH} (X = N, C) and the γ_{CH} modes at 852, 811, and 729 cm^{-1}, and if these modes are excluded from the analysis, a mean RHF deviation of about 12 cm^{-1} is obtained. Former RHF/3-21G or RHF/4-21G studies have resulted in mean deviations of 19 and 18 cm^{-1}, respectively.[16,17] It might be surprising that in the case of MP2 calculations, taking into account electron correlation, the mean frequency deviation increases as compared to the RHF level of calculation. It seems that this finding is typical for the results of MP2 calculations performed for heterocyclic compounds, e.g., pyridine and pyrimidine derivatives.[34]

The comparison of the overall shape of the predicted and the experimental spectra including the relative intensities of the bands leads to an even more convincing conclusion than that based on simple inspection of the mean frequency deviation. Figure 2 illustrates that the spectrum predicted at the DFT/B3LYP level is very similar to the experimental one in the fingerprint region, while the spectra simulated at the MP2 or RHF level differ more from the experimental one. In methods where the potential energy surface (PES) is corrected for the electron correlation, such as DFT and MP2, anharmonicity may become a more significant relative contributor to the overall error in the frequency prediction. Because the anharmonicity contributions are not uniform over the range of the vibrational modes of a polyatomic molecule, a uniform scaling procedure is less appropriate for a method whose most significant error rests in the anharmonicity of the vibrations and not in the

TABLE 8: Experimental (Ar Matrix) and Calculated (RHF, MP2, DFT/6-31++G) Vibrational Data for Water and Imidazole in the 1:1 H-Bonded Complex N_4···HO−H**

expt		calcd									optimal scaling factor[f]			PED[g]			
		ν^b (cm^{-1})			$\Delta\nu^a$ (cm^{-1})			I (km/mol)									
ν (cm^{-1})	$\Delta\nu^a$ (cm^{-1})	RHF[c]	MP2[d]	DFT[e]	RHF	MP2	DFT	RHF	MP2	DFT	RHF	MP2	DFT		RHF	MP2	DFT
								Water Vibrations									
3702	−34	4231	3955	3883	−38	−55	−47	137	105	73	0.875	0.936	0.953	ν^f_{OH}	78	72	66
														ν^b_{OH}	22	28	34
3394	−244	4031	3649	3544	−116	−214	−263	455	707	860	0.842	0.930	0.958	ν^b_{OH}	78	72	66
														ν^f_{OH}	22	28	34
1617?	+26	1771	1669	1643	+42	+50	+43	85	52	51	0.913	0.969	0.984	δ(HOH)	100	88	87
														N···HO wag		10	10
580?		650	718	722	146	102	98				0.892	0.808	0.803	δ(N···HO)[f]	68	84	83
														N···HO wag	25	16	18
h		342	371	382	117	114	107							N···HO wag	63	80	78
														ν(N···HO)	33	12	12
														δ(HOH)		12	12
h		136	158	155	1.4	3	3							ν(N···HO)	98	97	98
h		103	125	111	140	135	130							···HO tors.	99	100	99
h		43	43	46	5	6	4							oop butterfly	105	105	106
h		23	25	30	11	8	10							ip butterfly	98	101	100
								Imidazole Vibrations									
3503	+1	3532	3572	3559	−3	−3	+1	118	80	66	0.891	0.934	0.953	$\nu(N_1H)$	100	100	100
i		3115	3228	3197	+2	+2	+5	2	<1	1				$\nu(C_2H)$	78	76	83
														$\nu(C_3H)$	21	21	15
i		3091	3212	3178	+4	+5	+14	2	2	2				$\nu(C_3H)$	43		
														$\nu(C_5H)$	41	97	97
														$\nu(C_2H)$	15		
i		3090	3205	3171	+4	−3	+7	3	2	3				$\nu(C_5H)$	58		
														$\nu(C_3H)$	36	78	83
														$\nu(C_2H)$		21	15
1528[j]	+6	1559	1504	1522	+2	+6	+6	26	7	14				$\nu(N_4C_5)$	34	25	25
														$\nu(C_2C_3)$	27	41	34
														$\delta(N_1H)$	13	17	16
														$\delta(C_3H)$	12	14	13
1490	+7	1492	1472	1468	+5	+8	+7	37	38	33				$\nu(C_2C_3)$	24		
														$\delta(C_2H)$	20	14	18
														$\delta(C_5H)$	18	25	21
														$\nu(N_4C_5)$	15	27	21
														$\nu(C_5N_1)$	13	20	14
1414	+7	1425	1431	1403	+5	+4	+8	29	16	17				$\delta(N_1H)$	41	27	37
														$\nu(C_5N_1)$	20	17	21
														$\nu(C_2C_3)$	14		12
														$\nu(N_1C_2)$	11	31	17
1330[j]	−3	1346	1343	1336	−1	+4	+3	10	8	6				$\nu(N_4C_5)$	32	24	31
														$\delta(C_3H)$	21	23	22
														$\nu(C_3N_4)$	16	25	21
														$\nu(N_1C_2)$	13		10
														$\delta(C_2H)$	11	10	
1242	−14	1266	1246	1236	+2	+1	−11	1	2	1				$\delta(C_5H)$	46	44	46
														$\delta(C_3H)$	21	22	22
														$\delta(C_2H)$	12		10
														$\nu(N_4C_5)$	12	17	13
1117?	*i*	1130	1129	1119	+5	+7	+3	4	2	4				$\nu(C_5N_1)$	27	31	18
														$\delta(C_2H)$	18	14	11
														$\nu(C_2C_3)$	15		
														$\delta(C_3H)$	12		15
														$\delta(N_1H)$		23	18
														$\delta(C_5H)$		13	13
1103	0	1108	1147	1137	0	+4	+5	8	4	5				$\nu(C_3N_4)$	55	53	50
														$\nu(N_1C_2)$	18	28	18
1089/1082		1071	1080	1072	+6	+3	+6	15	26	21				$\nu(C_5N_1)$	26		17
+7/+6														$\delta(C_3H)$	19	26	22
														$\nu(C_2C_3)$	15	20	18
														$\delta(N_1H)$	15	19	20
														$\delta(C_2H)$	11	11	
1061	+2	1038	1058	1048	+1	+4	+3	64	38	49				$\nu(N_1C_2)$	49	21	33
														$\delta(C_2H)$	19	31	26
														$\nu(C_5N_1)$		12	
														$\delta(C_3H)$		11	
														$\delta(C_5H)$			11
i		917	902	915	+4	+1	+3	2	2	1				δ_{R1}	83	87	83
i		902	753	841	+3	+2	0	<1	50	5				$\gamma(C_3H)$	50	103	91
														$\gamma(C_5H)$	38		
														$\gamma(C_2H)$	21		17
867	+15	899	876	889	+15	+13	+12	10	9	11				δ_{R2}	86	87	85
820	+9	879	723	792	+9	+13	+8	21	38	37				$\gamma(C_5H)$	65	95	97

TABLE 8: (Continued)

expt		calcd												PED[g]			
		ν^b (cm^{-1})			$\Delta\nu^a$ (cm^{-1})			I (km/mol)			optimal scaling factor[f]						
ν (cm^{-1})	$\Delta\nu^a$ (cm^{-1})	RHF[c]	MP2[d]	DFT[e]	RHF	MP2	DFT	RHF	MP2	DFT	RHF	MP2	DFT		RHF	MP2	DFT
								Imidazole Vibrations									
736	+7	756	649	708	+4	+4	+6	70	20	45				$\gamma(C_2H)$	80	59	87
														$\gamma(C_3H)$	18		
														τ_{R2}		30	
660[j]	−4	655	637	654	+1	+6	−2	18	43	3				τ_{R2}	81		69
														τ_{R1}	19	56	30
														$\gamma(C_2H)$		21	
640/632		618	584	621	0	+8	+1	12	1	15				τ_{R1}	74	23	60
+3/+2														τ_{R2}	25	57	36
568/543														$\gamma(N_1H)$	90	74	85
+15/+21		515	467	523	+18	+35	+21	130	65	95				τ_{R1}	12	28	18

[a] Experimental shifts are calculated with respect to monomer frequencies, and calculated shifts are calculated with respect to calculated monomer frequencies. [b] Water modes unscaled, base modes uniformely scaled. [c] Scaling factor 0.90. [d] Scaling factor 0.96. [e] Scaling factor 0.97. [f] Optimal scaling factor = ν^{exp}/ν^{calc}. [g] Only contributions ≥10 are listed. [h] Situated below observed region (<400 cm^{-1}). [i] Too weak to be observed experimentally or to be assigned with confidence. [j] Overlaps with a band due to the N—H···OH_2 complex.

TABLE 9: Experimental (Ar Matrix) and Calculated (RHF, MP2, or DFT/6-31G) Vibrational Data for Water and Imidazole in the 1:1 H-Bonded Complex N_4···HO—H**

expt		calcd												PED[g]			
		ν^b (cm^{-1})			$\Delta\nu^a$ (cm^{-1})			I (km/mol)			optimal scaling factor[f]						
ν (cm^{-1})	$\Delta\nu^a$ (cm^{-1})	RHF[c]	MP2[d]	DFT[e]	RHF	MP2	DFT	RHF	MP2	DFT	RHF	MP2	DFT		RHF	MP2	DFT
								Water Vibrations									
3702		4226	3974	3865	−42	−57	−54	104	73	44	0.875	0.936	0.953	ν^f_{OH}	82	77	70
														ν^b_{OH}	18	23	30
3394	−244	4067	3758	3637	−84	−134	−161	250	287	56	0.842	0.930	0.958	ν^b_{OH}	82	76	70
														ν^f_{OH}	18	23	29
1617?	+26	1802	1715	1696	+15	+33	+31	91	71	67	0.913	0.969	0.984	δ(HOH)	93	91	90
580?		653	708	702				283	219	277	0.892	0.808	0.803	δ(N···HO)[f]	92	77	94
h		306	312	318				107	89	79				N···HO wag	81	87	91
h		182	215	228				117	106	99				···HO tors	96	102	104
h		150	172	175				3	2	2				ν(N···HO)	99	102	101
h		67	94	89				16	16	16				ip butterfly	100	101	101
h		57	64	68				5	4	4				oop butterfly	111	113	112
								Imidazole Vibrations									
3503	+1	3537	3590	3562	−1	0	+2	104	87	364	0.891	0.934	0.953	$\nu(N_1H)$	100	99	100
i		3113	3235	3196	+3	+3	+5	107	2	3				$\nu(C_2H)$	80	80	85
														$\nu(C_3H)$	18	17	15
i		3093	3222	3181	+14	+15	+19	54	3	3				$\nu(C_5H)$	97	97	98
i		3086	3209	3167	+4	+6	+7	61	3	4				$\nu(C_3H)$	80	83	87
														$\nu(C_2H)$	18	17	13
1528[j]	+6	1568	1515	1529	−1	+4	+3	23	8	11				$\nu(N_4C_5)$	33	11	22
														$\nu(C_2C_3)$	31	44	39
														$\delta(N_1H)$	12	16	15
														$\delta(C_3H)$	12	13	13
1490	+7	1501	1482	1473	+3	+2	+1	30	24	20				$\nu(C_2C_3)$	24		14
														$\delta(C_2H)$	20	12	18
														$\delta(C_5H)$	18	23	20
														$\nu(N_4C_5)$	18	30	25
														$\nu(C_5N_1)$	13	23	15
1414	+7	1433	1445	1410	+6	+3	+5	11	15	16				$\delta(N_1H)$	42	26	37
														$\nu(C_5N_1)$	22	15	22
														$\nu(C_2C_3)$	12	11	12
														$\nu(N_1C_2)$	12	33	18
1330[j]	−3	1351	1352	1342	−3	+5	+2	2	12	9				$\nu(N_4C_5)$	32	25	32
														$\delta(C_3H)$	20	22	21
														$\nu(C_3N_4)$	17	25	21
														$\nu(N_1C_2)$	13		10
														$\delta(C_2H)$	11		10
1242	−14	1268	1248	1245	+1	−4	−7	4	2	2				$\delta(C_5H)$	46	44	44
														$\delta(C_3H)$	22	22	3
														$\nu(N_4C_5)$		16	12
1117?	*i*	1133	1135	1121	+5	+6	+2	8	1	3				$\nu(C_5N_1)$	26	29	16
														$\delta(C_2H)$	18	14	3
														$\nu(C_2C_3)$	15		
														$\delta(C_3H)$	13	10	15
														$\delta(N_1H)$		23	17
														$\delta(C_5H)$		15	14
1103	0	1111	1156	1143	+2	+4	+7	13	5	6				$\nu(C_3N_4)$	56	53	53
														$\nu(N_1C_2)$	18	28	20
														$\nu(C_5N_1)$			12

TABLE 9: (Continued)

expt		calcd ν^b (cm^{-1})			calcd $\Delta\nu^a$ (cm^{-1})			calcd I (km/mol)			optimal scaling factor[f]			PED[g]			
ν (cm^{-1})	$\Delta\nu^a$ (cm^{-1})	RHF[c]	MP2[d]	DFT[e]	RHF	MP2	DFT	RHF	MP2	DFT	RHF	MP2	DFT		RHF	MP2	DFT
							Imidazole Vibrations										
1089/1082	+7/+6	1074	1085	1075	+6	+2	+6	61	22	17				$\nu(C_5N_1)$	26		17
														$\delta(C_3H)$	19	26	20
														$\nu(C_2C_3)$	14	19	17
														$\delta(N_1H)$	15	19	20
														$\nu(N_1C_2)$		10	
1061	+2	1040	1063	1049	0	+2	0	1	33	45				$\nu(N_1C_2)$	49	21	32
														$\delta(C_2H)$	19	32	26
														$\nu(C_5N_1)$		10	
														$\delta(C_5H)$		12	13
														$\nu(C_3N_4)$		10	
i		919	905	915	+1	+1	0	2	1	1				δ_{R1}	84	88	86
i		913	790	841	+10	−4	+4	13	6	1				$\gamma(C_3H)$	25	92	80
														$\gamma(C_5H)$	69	11	16
														$\gamma(C_2H)$	13		
867	+15	893	876	888	+7	+10	+11	12	19	22				δ_{R2}	86	87	85
820	+9	889	782	819	+17	+36	+37	47	45	27				$\gamma(C_5H)$	35	93	90
														$\gamma(C_3H)$	62	14	18
736	+7	760	678	709	+2	+7	+6	14	85	29				$\gamma(C_2H)$	81	76	90
														$\gamma(C_3H)$	17		
660[j]	−4	661	660	664	+1	+3	+1	10	1	2				τ_{R2}	78	41	66
														τ_{R1}	24	55	37
														$\gamma(N_1H)$		11	
640/632	+3/+2	624	613	629	+1	+1	+4	283	43	17				τ_{R1}	73	24	45
														τ_{R2}	30	67	58
														$\gamma(N_1H)$		18	
568/543	+15/+21	587	527	522	+95	+22	+22	142	75	97				$\gamma(N_1H)$	92	71	88
														τ_{R1}		32	14

[a] Shift with respect to experimental or calculated monomer frequencies. Calculated water $\nu_3 - \nu_1 - \nu_2$ frequencies are 4268 − 4151 − 1787 (RHF), 4031 − 3892 − 1682 (MP2), and 3798 − 3911 − 1665 (DFT). [b−j] See Table 8.

TABLE 10: Experimental (Ar Matrix) and Calculated (RHF, MP2, or DFT/6-31++G) Vibrational Data for Water and Imidazole in the 1:1 H-Bonded Complex N_1—H···OH_2

expt		calcd ν^b (cm^{-1})			calcd $\Delta\nu^a$ (cm^{-1})			calcd I (km/mol)			optimal scaling factor[f]			PED[g]			
ν (cm^{-1})	$\Delta\nu$ (cm^{-1})	RHF[c]	MP2[d]	DFT[e]	RHF	MP2	DFT	RHF	MP2	DFT	RHF	MP2	DFT		RHF	MP2	DFT
							Water Vibrations										
3725	−11	4259	3997	3930	−10	−13	0	127	103	92	0.875	0.932	0.948	ν^a(HOH)	100	100	100
3632	−6	4142	3856	3812	−5	−7	+5	39	17	15	0.877	0.942	0.953	ν^s(HOH)	100	100	100
1627?	+26	1747	1646	1621	+18	+27	+21	121	91	87	0.914	0.970	0.985	δ(HOH)	99	97	95
h		243	250	247				59	48	47				H_2O oop transl.[f]	44	45	44
														H_2O ip wag	44	44	44
														ip butterfly	11	11	11
h		133	158	147				2	3	4				ν(N—H···O)	99	99	99
h		103	114	94				<1	2	4				H_2O twist	100	100	95
h		156	107	86				326	296	286				H_2O ip wag	44	49	47
														H_2O oop transl	49	48	46
h		59	60	59				1	1	2				ip butterfly	94	98	89
h		43	47	51				1	1	1				oop butterfly	98	100	97
							Imidazole Vibrations										
3373	−127	3463	3467	3434	−72	−108	−124	435	547	530	0.877	0.934	0.953	$\nu(N_1H)$	99	99	99
i		3109	3222	3188	−2	−4	0	3	2	2				$\nu(C_2H)$	80	80	86
														$\nu(C_3H)$	18	18	12
i		3084	3204	3164	−3	−4	−4	1	2	2				$\nu(C_5H)$	83	97	96
														$\nu(C_3H)$	10		
i		3082	3196	3159	−5	−6	−5	10	4	6				$\nu(C_3H)$	71	81	86
														$\nu(C_5H)$	15		
														$\nu(C_2H)$	14	18	11
1528[j]	+6	1558	1507	1520	+1	+9	+4	24	9	13				$\nu(N_4C_5)$	32		21
														$\nu(C_2C_3)$	24	31	28
														$\delta(N_1H)$	20	35	28
														$\delta(C_3H)$	11	10	11
1494	+11	1491	1468	1474	+4	+4	+13	34	25	23				$\delta(C_2H)$	20	14	19
														$\nu(C_2C_3)$	19		15
														$\delta(C_5H)$	18	26	22
														$\nu(C_5N_1)$	16	17	14
														$\nu(N_4C_5)$	15	27	20
1437/1431		1439	1443	1417	+19	+16	+22	20	15	13				$\delta(N_1H)$	40	23	37
+22/+24														$\nu(C_2C_3)$	21	21	19

TABLE 10: (Continued)

expt		calcd ν^b (cm^{-1})			calcd $\Delta\nu^a$ (cm^{-1})			calcd I (km/mol)			optimal scaling factor[f]			PED[g]			
ν (cm^{-1})	$\Delta\nu$ (cm^{-1})	RHF[c]	MP2[d]	DFT[e]	RHF	MP2	DFT	RHF	MP2	DFT	RHF	MP2	DFT		RHF	MP2	DFT
							Imidazole Vibrations										
														$\nu(C_5N_1)$	12	14	14
														$\nu(N_1C_2)$	11	22	13
1330[j]	−3	1344	1340	1330	−3	+1	−3	12	10	9				$\nu(N_4C_5)$	33	23	31
														$\delta(C_3H)$	22	26	23
														$\nu(C_3N_4)$	16	26	18
														$\nu(N_1C_2)$	12		11
1257	+1	1264	1243	1247	0	−2	0	2	2	1				$\delta(C_5H)$	45	42	45
														$\delta(C_3H)$	20	20	20
														$\nu(N_4C_5)$	13	20	16
1140	+16	1133	1140	1133	+8	+18	+17	4	4	2				$\nu(C_5N_1)$	39	39	41
														$\delta(C_5H)$	14		15
														$\delta(N_1H)$	13		
														$\delta(C_2H)$	13		
														$\nu(C_3N_4)$		21	
														$\delta(C_3H)$			12
i		1116	1156	1137	+8	+13	+5	2	<1	2				$\nu(C_3N_4)$	53	28	58
														$\nu(N_1C_2)$	29	12	32
														$\delta(N_1H)$		18	
1089	+13	1076	1088	1082	+11	+11	+16	20	23	22				$\delta(C_3H)$	29	35	33
														$\nu(C2C_3)$	17	22	20
														$\nu(C_3N_4)$	16		
														$\nu(C_5N_1)$	13		
														$\nu(N_1C_2)$		12	12
1065	+6	1044	1100	1049	+7	+46	+4	54	26	34				$\nu(N_1C_2)$	38	13	20
														$\delta(C_2H)$	27	37	34
														$\nu(C_5N_1)$		13	13
														$\nu(C_3N_4)$		10	
														$\delta(C_5H)$			10
i		916	900	912	+3	−1	0	<1	<1	<1				δ_{R1}	84	86	58
i		898	738	839	−1	−13	−2	<1	12	23				$\gamma(C_3H)$	55	95	84
														$\gamma(C_5H)$	32		15
														$\gamma(C_2H)$	21		
860	+8	889	871	884	+5	+8	+7	6	5	7				δ_{R2}	88	88	87
813	+2	872	712	792	+2	+2	+8	25	33	102				$\gamma(C_5H)$	71	94	52
														$\gamma(C_3H)$	32		
														$\gamma(N_1H)$			29
														$\gamma(C_2H)$		12	
736[j]	+7	760	647	710	+8	+2	+8	121	8	35				$\gamma(C_2H)$	70	66	88
														$\gamma(C_3H)$	13		
														τ_{R2}		29	
770																	
+217/+248		736	807	784	+239	+375	+282	35	133	4				$\gamma(N_1H)$	75		
														$\gamma(C_2H)$	11	66	88
														$\gamma(C_3H)$			14
660[j]	−4	651	612	652	−3	−19	−4	42	5	25				τ_{R2}	102	15	102
														τ_{R1}		90	
618/612/606		594	534	596	−24	−42	−24	43	42	19				τ_{R1}	97	20	100
−21/−24/−24														τ_{R2}		64	
														$\gamma(C_2H)$		21	

[a−i] See Table 8.

accounting for the electron correlation effects. Therefore, a single scaling factor is less appropriate for correlated methods than for the RHF method. This explains the larger mean deviations obtained with the DFT and MP2 methods than with the RHF method, in which a single scaling factor is used. For the correlated methods, the use of different scaling factors for different vibrational modes, reflecting the differences in anharmonicity, will be relatively more important than for a noncorrelated method such as RHF.

For example, when different scaling factors are used for the DFT frequency predictions, e.g., 0.975 for all modes, except ν_{XH} and γ_R modes for which scaling factors of 0.950 and 0.980 are used, respectively, the mean frequency deviation decreases to 10 cm^{-1}. When the same procedure is applied to the MP2-predicted frequencies, by use of a scaling factor of 0.960 for all modes except the ν_{XH} (0.930) modes and the γ_{XH} and γ_R modes (1.00), the mean deviation decreases only to 23 cm^{-1}. The use of different scaling factors for frequencies belonging to different types of vibrational modes seems imminent in this case, and it has been proposed by several authors.[8,35]

On inspection of Tables 3 and 4, we can compare the PED analysis at different levels of theory. The differences between the DFT and MP2 PED's are smaller than between the RHF and DFT, and RHF and MP2. For some of the vibrational modes, particularly for those with comparable frequencies, the main internal mode contribution is often different for different methods. In consequence, the assignment varies with the level of theory and it is difficult to determine which method gives the most reliable result. This feature has also been noted by others in the DFT study on cytosine.[13] For the vibrational modes with frequencies at 1124 and 1103, and at 893 and 852 cm^{-1}, a conclusive assignment is difficult but most probably the DFT method gives the best description.

The RHF method provides much higher values of absolute intensities of the IR modes than the MP2 and the DFT methods. Probably the former values are seriously overestimated. Both

TABLE 11: Experimental (Ar Matrix) and Calculated (RHF, MP2 or DFT/6-31G) Vibrational Data for Water and Imidazole in the 1:1 H-Bonded Complex N_1—H···OH_2**

expt		calcd									optimal scaling factor[f]			PED[g]			
		ν^b (cm^{-1})			$\Delta\nu^a$ (cm^{-1})			I (km/mol)									
ν (cm^{-1})	$\Delta\nu$ (cm^{-1})	RHF[c]	MP2[d]	DFT[e]	RHF	MP2	DFT	RHF	MP2	DFT	RHF	MP2	DFT		RHF	MP2	DFT
								Water Vibrations									
3725	−11	4264	4020	3915	−4	−11	+4	99	70	53	0.874	0.927	0.951	ν^a(HOH)	100	100	100
3632	−6	4148	3886	3803	−3	−6	+5	37	19	13	0.876	0.935	0.955	ν^s(HOH)	100	100	100
1617?	+26	1765	1674	1652	−22	−8	−13	94	69	62	0.904	0.953	0.966	δ(HOH)	98	98	98
h		234	275	290				60	15	7				H_2O oop transl.[f]	44	45	45
														H_2O ip wag	44	44	45
														ip butterfly	13		
h		83	205	237				308	274	271				H_2O ip wag	44	47	48
														H_2O oop transl.	44	46	48
h		138	160	164				2	2	4				ν(N—H···O)	99	98	99
h		95	87	86				2	38	43				H_2O twist	99	59	55
														ip butterfly		41	45
h		56	53	53				2	18	19				ip butterfly	91	57	54
														H_2O twist		40	44
														oop butterfly	89	97	97
								Imidazole Vibrations									
3373	−127	3455	3438	3376	−83	1524	−184	453	597	623	0.879	0.942	0.969	$\nu(N_1H)$	99	99	99
i		3107	3228	3188	−23	−4	−3	6	2	3				$\nu(C_2H)$	83	85	89
														$\nu(C_3H)$	15	13	10
i		3078	3198	3155	−4	−5	−5	<1	11	1				$\nu(C_5H)$	44	37	33
														$\nu(C_3H)$	44	56	58
														$\nu(C_2H)$	11		
i		3076	3200	3152	−3	−7	−10	18	<1	16				$\nu(C_3H)$	40	30	32
														$\nu(C_5H)$	55	62	66
														$\nu(C_2H)$	14	18	11
1528[j]	+6	1558	1507	1520	+1	+9	+4	24	9	13				$\nu(N_4C_5)$	32		19
														$\nu(C_2C_3)$	26	30	29
														$\delta(N_1H)$	18	37	28
														$\delta(C_3H)$	11	10	11
1494	+11	1502	1486	1478	+4	+6	+6	30	19	20				$\delta(C_2H)$	19	12	18
														$\nu(C_2C_3)$	20		13
														$\delta(C_5H)$	18	26	22
														$\nu(C_5N_1)$	16	20	15
														$\nu(N_4C_5)$	17	29	22
1437/1431		1439	1443	1417	+19	+16	+22	20	15	13				$\delta(N_1H)$	42	22	37
+22/+24														$\nu(C_2C_3)$	19	24	20
														$\nu(C_5N_1)$	14	11	13
														$\nu(N_1C_2)$	11	24	13
1330[j]	−3	1350	1352	1337	−4	+5	−3	13	13	13				$\nu(N_4C_5)$	32	22	31
														$\delta(C_3H)$	22	26	24
														$\nu(C_3N_4)$	16	23	18
														$\nu(N_1C_2)$	12		11
														$\delta(C_2H)$	11		
1257	+1	1267	1251	1253	0	−1	+1	1	2	1				$\delta(C_5H)$	45	42	44
														$\delta(C_3H)$	20	19	20
														$\nu(N_4C_5)$	13	22	17
														$\delta(C_2H)$	10		
1140	+16	1138	1150	1142	+10	+21	+23	3	4	3				$\nu(C_5N_1)$	38	36	41
														$\delta(C_5H)$	15		
														$\delta(N_1H)$	13		
														$\delta(C_2H)$	14		
														$\nu(C_3N_4)$		27	17
i		1120	1169	1143	+11	+17	+7	2	<1	<1				$\nu(C_3N_4)$	54	23	41
														$\nu(N_1C_2)$	30	30	36
														$\delta(N_1H)$		18	11
1089	+13	1081	1097	1082	+13	+14	+13	15	17	17				$\delta(C_3H)$	29	37	36
														$\nu(C2C_3)$	16	21	20
														$\nu(C_3N_4)$	17		
														$\nu(C_5N_1)$	13		
														$\nu(N_1C_2)$		11	11
1065	+6	1047	1063	1049	+7	+2	0	50	20	27				$\nu(N_1C_2)$	38	13	19
														$\delta(C_2H)$	27	38	35
														$\nu(C_5N_1)$		13	13
														$\nu(C_3N_4)$		10	
														$\delta(C_5H)$	10		
i		919	903	912	+1	1−1	30	<1	1	2				δ_{R1}	84	87	85
i		900	781	792	−3	−13	−45	<1	<1	33				$\gamma(C_3H)$	56	98	44
														$\gamma(C_5H)$	31		
														$\gamma(C_2H)$	21		
														$\gamma(N_1H)$			38
860	+8	891	875	884	+5	+9	+7	8	9	9				δ_{R2}	88	88	88
813	+2	872	743	784	0	−3	+2	16	31	17				$\gamma(C_5H)$	72	97	92

TABLE 11: (Continued)

expt		calcd								optimal scaling factor[f]			PED[g]			
		ν^b (cm^{-1})			$\Delta\nu^a$ (cm^{-1})			I (km/mol)								
ν (cm^{-1})	$\Delta\nu$ (cm^{-1})	RHF[c]	MP2[d]	DFT[e]	RHF	MP2	DFT	RHF	MP2	DFT	RHF	MP2	DFT		RHF	MP2	DFT
Imidazole Vibrations																	
														$\gamma(C_3H)$	32		
														$\gamma(C_2H)$		12	
736[j]	+7	764	676	710	+6	+5	+7	91	12	18				$\gamma(C_2H)$	71	85	86
														$\gamma(C_3H)$	11		10
														$\gamma(C_5H)$		11	10
770		741	847	839	+249	+342	+339	46	114	62				$\gamma(N_1H)$	73	85	86
+217/+248														$\gamma(C_2H)$	11		
														$\gamma(C_3H)$			47
660[j]	−4	656	644	652	−4	−13	−11	43	26	21				τ_{R2}	102	88	101
														τ_{R1}		19	
618/612/606		599	588	596	−24	−24	−29	43	5	12				τ_{R1}	96	94	110
−21/−24/−24														τ_{R2}		18	11
														$\gamma(N_1H)$	11		

[a−i] See Table 9.

calculations, which take into account electron correlation effects (MP2 and DFT), give similar magnitudes of the absolute intensities. The relative intensities of the absorption bands in the spectrum predicted by the DFT method are closest to the relative intensities measured in the experimental spectrum.

Comparison of Tables 3 and 4 demonstrates the basis set dependence of the frequency calculations (6-31++G** and 6-31G**). Slightly better results, in terms of mean deviations, are obtained for the SCF and DFT methods with the larger basis set. Surprisingly, the opposite is true for the MP2 method.

H-Bonded Complexes with H_2O. Two H-bonded complex structures of IM are considered in this work: the N_1—H···OH_2 and N_4···H—OH structures. The optimized geometries of these structures are shown in Scheme 1. Tables 5 and 6 summarize the results of the energy calculations for the H-bonded complexes at all levels of theory employed. All three levels of theory, predict the N_4···H—OH and N_1—H···OH_2 water complex as being equally stable. The differences in relative energy, ΔE, of the N_4···H—OH and the N_1—H···OH_2 complex are very small: 0.22 (MP2/6-31++G**//SCF/6-31++G**), 0.04 (MP2/6-31++G**), and 2.17 (DFT/6-31++G**) kJ/mol.

The H-bond interaction energies for the two complexes range from 19 to 30 kJ/mol, depending on the method employed. The H-bond interaction energies are the lowest for the RHF method and the highest for the MP2 method. The BSSE error is evaluated at 6 kJ/mol for the MP2 method and at 2 kJ/mol for the RHF method. The MP2//MP2 interaction energies correspond very well with the interaction energies obtained at the MP2//RHF level, with the maximum difference being only 2 kJ/mol. The differences in interaction energies originate mainly from the contribution of the dispersion term in the total interaction energy. The dispersion term is not accounted for at the RHF level and, from the difference in interaction energies at the RHF and MP2 levels, can be estimated at 4−5 kJ/mol for the IM·water complexes.

The present results can be compared with the recent data published by Nagy *et al.*[20] With the slightly more extended basis set (6-311++G**) at the MP2 + ZPE level, the value of the H-bond interaction energy for the N_1—H···OH_2 complex obtained by these authors is extremely close to the value of the present work. However, a rather large deviation is found for the N_4···HO—H complex of IM. In our opinion, the significantly smaller value quoted by Nagy *et al.* for this structure is due in part to their large difference (about 3.1 kJ/mol) from the ΔZPE contribution between the two isomeric complexes. Such a large ZPE difference is difficult to understand for isomeric H-bonded complexes where only the intermolecular modes can differ more significantly. As a matter of fact, this ΔZPE term amounts to only 1.7 kJ/mol in our calculations. We therefore consider the value for the N_4···HO—H complex of IM listed in the tables by Nagy *et al.* as questionable. A reliable comparison between the BSSE-corrected interaction energies is more difficult, since the numbers quoted by Nagy *et al.* have been obtained with the less extended basis set 6-31G*. Nevertheless, the agreement for the N_1—H···OH_2 structure is again rather good, while the value for the N_4···HO—H complex may be affected by the same ΔZPE problem mentioned above.

The predicted water bond distance is about ±0.02 Å shorter at the RHF level than for the MP2 and DFT methods. The H-bond distances (N···O) for the two complexes are ±0.1 Å higher at the RHF level than for MP2 and DFT. The shorter H-bond distances for the MP2 and DFT methods can be explained by a better description of all terms contributing to the H-bond energy and the account for dispersion energy contributions.

The FTIR spectrum of IM/H_2O/Ar is shown in Figures 3 and 4. Two strong complex bands appear in the region below the NH stretch at 3394 and 3373 cm^{-1}, respectively. If, as can be expected from the energy calculations listed in Tables 5 and 6, both the N_1—H···OH_2 and the N_4···HO—H complex species will be present in the matrix sample, a shifted ν_{NH} mode and a rather strongly shifted water ν^b_{OH} mode should be observed in that spectral region. In view of the proton affinity (PA) value of 930 kJ/mol for IM[36] and the correlation relating $\Delta\nu^b_{OH}$ to PA_B established earlier for some N···HO—H complexes in Ar,[2,33,37] the ν^b_{OH} mode for water acting as a proton donor in the N···HO—H complex with IM is expected to be near 3400 cm^{-1}. However, the closeness of the complex bands at 3394 and 3373 cm^{-1} does not allow assignment of the former to the ν^b_{OH} mode using the above argument alone, and deuteration experiments have been performed to discriminate between the two bands. The presence of the two complex species, N—H···OH_2 and N···HO—H, is also manifested by the appearance of two shifted water ν_3 bands in the spectrum shown in Figure 3 at 3725 and 3702 cm^{-1}, respectively. The former frequency is the same as that assigned to the water acceptor ν_3 mode for the N—H···OH_2 complex of pyrrole[23] and is also close to the 3724 and 3721 cm^{-1} for the O—H···OH_2 complexes of 3- and 4-hydroxypyridine, respectively.[38,1d] The ν_3 mode observed at 3702 cm^{-1} is very close to the ν^f_{OH} frequency of water in the N···HO—H H-bonded structures of water with pyridine (3701) and with pyrimidine (3703),[1b] with 4-OH-pyridine (3703),[1d] and with 4-NH_2-pyridine (3702).[1c] A similar asymmetric, double frequency shift is also observed in the water

ν_2 region close to the water dimer acceptor mode (1593 cm^{-1})[39] at 1596 cm^{-1} and to the water dimer donor mode (1612 cm^{-1})[39] at 1617 cm^{-1} (Figure 4). The latter frequency is again not far from the proton-donor ν_2 mode in the N···HO—H complexes of water with pyridine (1616) and pyrimidine (1615)[1b] and with 4-OH-pyridine (1619).[1c] However, the former band is much less displaced from the monomer ν_2 band than predicted at all three levels of theory, and its assignment is questionable.

The results of two deuteration experiments are illustrated in Figures 5 and 6. The first spectrum is that of a sample of IM-d_4 (70%)/H_2O/Ar, which allows information to be obtained from both the ν_{NH} and the ν_{ND} spectral regions. The free ν_{ND} mode of the partially deuterated compound appears as an intense, triplet-split band at 2594/2588/2582 cm^{-1}. This yields the isotopic ratio (ISR) ν_{NH}/ν_{ND} value of 1.357. In the ν_{NH} spectral region of the water-doped sample (Figure 5), the complex band at 3394 cm^{-1} is much stronger than that at 3373 cm^{-1}. This is the first indication that the band at 3394 cm^{-1} is due to the ν^b_{OH} mode in the N_4···HO—H complex, while the band at 3373 cm^{-1} corresponds to the shifted ν_{NH} mode in N_1—H···OH_2. Further support for this assignment is obtained from the observation of the corresponding complex band ν_{ND}... in the ν_{ND} region at 2505 cm^{-1} yielding a quite acceptable ISR value of 1.347.

Although the spectrum of IM/D_2O/Ar (Figure 6) is somewhat complicated by isotopic exchange $D_2O \rightarrow$ HOD ($\rightarrow H_2O$), the band at 2493 cm^{-1} definitely does not correspond to a D_2O or HOD dimer, trimer, ... absorption.[39,33] It can only be assigned to the ν^b_{OD} mode of the N···DO—D(H) H-bonded structure, and its ISR value is 1.361. The ν_{NH} region of this spectrum shows a complex band at 3364 cm^{-1} and a very weak shoulder at 3373 cm^{-1}. The latter can be explained by the isotopic exchange of D_2O leading to a small amount of H_2O in the sample, which forms a small amount of N—H···OH_2 species. The bonded ν_{NH}... mode of the more abundant N—H···O—DD-(H) complex absorbs at a slightly lower frequency than that of the N—H···OH_2 complex, and this effect of isotopic fortification of an H-bond is well-known, e.g., for the water dimer (ν_{OD} for HOD···OH_2 at 2639 cm^{-1} but for HOD···OD_2 at 2635 cm^{-1}).[39] All the deuteration results allow us to unambiguously assign the complex band at 3394 cm^{-1} to the ν^b_{OH} mode in the N···HO—H species and the 3373 cm^{-1} feature to the ν_{NH} mode in the N—H···OH_2 species for the non-deuterated IM·H_2O complexes. The absorptions attributed above to the N_1—H···OH_2 and N_3···H—OH complexes are certainly not due to vibrations in the imidazole dimer. Dimerization of imidazole occurs above sublimation temperatures of 25 °C and is characterized by a broad absorption with a maximum around 2950 cm^{-1} in the high-frequency region.[23]

Relative Concentration of the N—H···OH_2 and N···HO—H Complexes. In order to compare the experimental data as accurately as possible with the theoretical predictions, intensity measurements for the two representative complex absorptions 3394 (ν^b_{OH}) and 3373 (ν_{N-H}...) cm^{-1} need to be performed for spectra where (i) preferably only 1:1 complexes are present in the matrix and (ii) the two nearby absorptions are clearly separated (this happens when the absorptions are rather weak). The first condition is difficult to fulfill in the case of water complexes, since this compound has a strong tendency for self-association and even at low matrix-to-solute ratios a small amount of water is always present. Nevertheless, a spectrum that satisfies quite well the two conditions has been obtained, and it is shown in Figure 3B. The relative concentration of the two complexes of IM with water calculated using experimental relative intensities (I) from this spectrum and the theoretically predicted intensities (a) (Tables 8−11) can be calculated as

$$[N_1\text{—H}\cdots OH_2]/[N_4\cdots\text{HO—H}] = (I(3373)/I(3394))(a(\nu^b_{OH})/a(\nu_{N-H}...))$$

Table 7 summarizes the results for the relative abundances of the two complexes. Rather large differences are obtained depending on the method employed. This is due to the expected, significant inaccuracy of the theoretical prediction of absolute intensities of the bands due to the vibrations of groups directly engaged in the H-bond interaction. The almost 1:1 ratio of the two complex species N_1—H···OH_2 and N_4···HO—H (obtained with the predicted intensities of the 6-31++G** basis set) is consistent with very small relative energies (Tables 5 and 6). Table 7 demonstrates the differences in the relative abundances calculated with the theoretical results obtained with the two basis sets employed. The predicted intensity of the ν^b_{OH} water mode in the N_4···H—OH complex is about 2 times higher for the 6-31++G** basis set than for the 6-31G** basis set. The better description of the frequency shift of this mode upon H-bonding (see Tables 8 and 10), with the diffuse functions added to the basis set, suggests that the results obtained with the 6-31++G** basis set are probably more reliable.

Although the interaction energies for the H-bond interaction between water and IM do not strongly depend on whether the basis set includes diffuse orbitals, the opposite is true for the predicted frequency shifts, especially for the normal modes directly influenced by the H-bond formation. Tables 8 to 11 summarize the experimental and theoretical vibrational data.

The most perturbed vibrational mode in the N_4···H—OH complex is the ν^b_{OH} water mode. The best account for the frequency shift of this mode is obtained with the MP2 and DFT methods with the 6-31++G** basis set. The improvement of the prediction of this frequency shift is remarkable when the diffuse functions are included in the basis set. A better description of the σ interaction of the lone pair of nitrogen with the molecular orbitals of water resulting from including diffuse orbitals is the likely reason for this improvement. One can also note the slightly better prediction of the frequency shifts of the IM vibrations by the DFT method. However, with a few exceptions only, rather good predictions are also obtained with the RHF/6-31++G** method.

The ν_{NH}, δ_{NH}, and γ_{NH} vibrations are the modes most perturbed by the formation of the N_1—H···OH_2 H-bonded complex. Also in this case, the best frequency shifts for the ν_{NH} mode are obtained with the MP2 and DFT methods with the 6-31++G** basis set. For the two other modes, it is difficult to indicate the best method, but here also, slightly better results are obtained when extra diffuse functions are added to the basis set. The relatively strong frequency increase predicted for the δ_{NH} mode in N_1—H···OH_2 is experimentally confirmed by the appearance of the complex band at 1437/1431 cm^{-1}, while a very large shift of the γ_{NH} mode is manifested by the rather broad absorption at 770 cm^{-1}. Such a large frequency perturbation of this internal IM mode is not anticipated based on the magnitude of the N_4···HO—H H-bonding interaction.

As far as the internal IM modes are concerned, rather weak frequency perturbations are observed for most ring stretches and CH deformations, and these can be identified by comparison with the *ab initio* spectral predictions (Tables 10 and 11). Also in this case, slightly better predictions for the IM mode shifts are obtained with the DFT/6-31++G** method.

Summary

Experimental matrix-isolation FTIR spectroscopy and *ab initio* theoretical calculations were applied to investigate the H-bonding interaction of water with IM. Formation of N_1—H···OH_2 complexes is manifested in the experimental

spectra by relatively strong perturbations of the NH stretching and in-plane and out-of-plane deformation modes and by weak perturbations of the bonded proton acceptor. On the other hand, the $N_4\cdots HO{-}H$ complex of IM, which is about equal in strength compared to the isomeric $N_1{-}H\cdots OH_2$ complex of this compound, induces stronger perturbations of the bonded water modes. Spectral features due to these two complexes can be distinguished by careful comparison with the *ab initio* predicted spectra. The DFT method with the basis set including diffuse functions yields considerably better frequency predictions for vibrational modes directly involved in the H-bond interactions, e.g., ν^{b}_{OH} for $N_4\cdots HO{-}H$ or ν_{NH} for $N_1{-}H\cdots OH_2$, and slightly better shift predictions for the internal IM modes.

Acknowledgment. This work was part of an ECC research project S&T Cooperation with Central and Eastern European Countries (ERB CIPA-CT 93-0108), and G. Maes and M. J. Nowak acknowledge support from the ECC Commission. The cooperation between the groups of Leuven and Tucson was supported by the NATO International Collaborative Grant INT-9313268. J. Smets acknowledges the support of the Belgian IWONL. L. Adamowicz and J. Smets acknowledge the support from the Office of Health and Environmental Research, Office of Basic Energy Research, Department of Energy (Grant No. DEFG0393ER61605). G. Maes also acknowledges the Belgian NFWO for a permanent research fellowship.

References and Notes

(1) (a) Smets, J.; Adamowicz, L.; Maes, G. *J. Mol. Struct.* **1994**, *322*, 113. (b) Destexhe, A.; Smets, J.; Adamowicz, L.; Maes, G. *J. Phys. Chem.* **1994**, *98*, 1506. (c) Smets, J.; Adamowicz, L.; Maes, G. *J. Phys. Chem.* **1995**, *99*, 6387. (d) Buyl, F.; Smets, J.; Maes, G.; Adamowicz, L. *J. Phys. Chem.* **1995**, *99*, 14697. (e) Smets, J.; Adamowicz, L.; Maes, G. *J. Phys. Chem.*, in press. (f) Smets, J.; Destexhe, A.; Adamowicz, L.; Maes, G. *J. Phys. Chem.*, submitted. (g) Smets, J.; Destexhe, A.; Adamowicz, L.; Maes, G. *J. Phys. Chem.*, submitted.

(2) Smets, J.; McCarthy, W.; Maes, G.; Adamowicz, L. *J. Am. Chem. Soc.*, submitted.

(3) Sim, F.; St-Amant, A.; Papai, I.; Salahub, D. R. *J. Am. Chem. Soc*. **1992**, *114*, 4391.

(4) Johnson, B. G.; Gill, P. M. W.; Pople, J. A. *J. Chem. Phys*. **1993**, *98*, 5612.

(5) Mijoule, C.; Latajka, Z.; Borgis, D. *Chem. Phys. Lett.* **1993**, *208*, 364.

(6) Latajka, Z.; Bouteiller, Y. *J. Chem. Phys.* **1994**, *101*, 9793.

(7) Kim, K.; Jordan, K. D. *J. Phys. Chem.* **1994**, *98*, 10089.

(8) Rauhut, G.; Pulay, P. *J. Phys. Chem*. **1995**, *99*, 3093.

(9) Del Bene, J. E.; Person, W. B.; Szczepaniak, K. *J. Phys. Chem*. **1995**, *99*, 10705.

(10) Barone, V.; Adamo, C. *J. Phys. Chem.* **1995**, *99*, 15062.

(11) Topol, I. A.; Burt, S. K.; Rashin, A. A. *Chem. Phys. Lett.* **1995**, *247*, 112.

(12) Adamo, C.; Lelj, F. *Int. J. Quantum Chem*. **1995**, *56*, 645.

(13) Kwiatkowski, J. S.; Leszczynski, J. *J. Phys. Chem.* **1996**, *100*, 941.

(14) Bellocq, A.; Perchard, C.; Novak, A.; Josien, M. *J. Chim. Phys. Phys.-Chim. Biol.* **1965**, *11/12*, 1334. Perchard, C.; Bellocq, A.; Novak, A. *J. Chim. Phys. Phys.-Chim. Biol.* **1965**, *11/12*, 1344.

(15) King, S. T. *J. Phys. Chem.* **1970**, *74*, 2133.

(16) Majoube, M.; Vergoten, G. *J. Mol. Struct.* **1992**, *266*, 345.

(17) Fan, K.; Xie, Y.; Boggs, J. E. *J. Mol. Struct.: THEOCHEM.* **1986**, *136*, 339.

(18) Zheng, Y.; Merz, K. M. *J. Comput. Chem.* **1992**, *13*, 1151.

(19) Alagona, G.; Ghio, C.; Nagy, P. I.; Simon, K.; Naray-Szabo, G. *J. Comput. Chem.* **1990**, *11*, 1038.

(20) Nagy, P. I.; Durant, G. J.; Smith, D. A. *J. Am. Chem. Soc.* **1993**, *115*, 2912.

(21) Maes, G. *Bull. Soc. Chim. Belg.* **1981**, *90*, 1093.

(22) Graindourze, M.; Smets, J.; Zeegers-Huyskens, Th.; Maes, G. *J. Mol. Struct.* **1990**, *222*, 345.

(23) Van Bael, M. K. M.Sc. Thesis, University of Leuven, Heverlee, Belgium, 1994.

(24) Szabo, A.; Ostlund, N. S. *Modern Quantum Chemistry*; McGraw-Hill: New York, 1989.

(25) Chatasinski, G.; Szczesniak, M. *Chem. Rev.* **1994**, *94*, 1723.

(26) Becke, A. D. *J. Chem. Phys.* **1993**, *98*, 5648.

(27) Parr, R. G.; Yang, W. *Density-functional Theory of Atoms and Molecules*; Oxford University Press: New York, 1989.

(28) Frisch, C. P. M. J.; Trucks, G. W.; Head-Gordon, M.; Gill, P. M. W.; Wong, W. M.; Foresman, J. B.; Johnson, B. G.; Schlegel, H. B.; Robb, M. A.; Replogie, E. S.; Gomperts, R.; Andres, J. L.; Raghavachari, K.; Binkley, J. S.; Gonzales, C.; Martin, R. L.; Fox, D. J.; Defrees, D. J.; Baker, J.; Stewart, J. J. P.; Pople, J. A. GAUSSIAN 92; Gaussian Inc.: Pittsburgh, PA, 1992. Frisch, C. P. M. J.; Trucks, G. W.; Schlegel, H. B.; Gill, P. M. W.; Johnson, B. G.; Robb, M. A.; Cheeseman, J. R.; Keith, T.; Petersson, G. A.; Montgomery, J. A.; Raghavachari, K.; Al-Laham, M. A.; Zakrzewski, V. G.; Ortiz, J. V.; Foresman, J. B.; Peng, C. Y.; Ayala, P. Y.; Chen, W.; Wong, M. W.; Andres, J. L.; Replogle, E. S.; Gomperts, R.; Martin, R. L.; Fox, D. J.; Binkley, J. S.; Defrees, D. J.; Baker, J.; Stewart, J. P.; Head-Gordon, M.; Gonzales, C.; Pople, J. A. GAUSSIAN 94; Revision B.3; Gaussian Inc.: Pittsburgh, PA, 1995.

(29) Califano, S. *Vibrational States*; Wiley: New York, 1976.

(30) Boys, S. F.; Benardi, F. *Mol. Phys.* **1970**, *19*, 553.

(31) Van Duijneveldt, F. B.; van Duijneveldt- van de Rijdt, J. G. C. M.; van Leuthe, J. H. *Chem. Rev.* **1994**, *94*, 1973.

(32) Christen, D.; Griffiths, J. H.; Sheridan, J. *Z. Naturforsch.* **1982**, *37A*, 1378.

(33) Smets, J. Ph.D. Thesis, University of Leuven, Heverlee, Belgium, 1993.

(34) Kwiatkowski, J. S.; Leszczynski, J.; Nowak, M.; Lapinski, L. To be published.

(35) Person, W. B.; Szczepaniak, K. *Vibrational Spectra and Structure*; Durig, J. R., Ed.; Elsevier: Amsterdam, 1993; Vol. 2, p 239.

(36) Lias, S. G.; Liebman, J. F.; Levin, R. D. *J. Phys. Chem. Ref. Data* **1984**, *13*, 695.

(37) Maes, G.; Smets J. *J. Mol. Struct.* **1992**, 270, 141.

(38) Person, W. B.; Del Bene, J. E.; Szajda, W.; Szczepaniak, K.; Szczesniak, M. *J. Phys. Chem.* **1991**, *95*, 2770.

(39) Engdahl, A.; Nelander, B. *J. Mol. Struct.* **1989**, *193*, 101.